MOLECULAR AND CELLULAR BIOLOGY, July 2001, p. 4785–4806 Vol. 21, No. 14
0270-7306/01/$04.00+0 DOI: 10.1128/MCB.21.14.4785–4806.2001

Insulin-Responsive Compartments Containing GLUT4 in 3T3-L1 and CHO Cells: Regulation by Amino Acid Concentrations

JONATHAN S. BOGAN,[1,2] ADRIENNE E. MCKEE,[2] AND HARVEY F. LODISH[2,3]*

Diabetes Unit, Department of Medicine, Massachusetts General Hospital and Harvard Medical School, Boston, Massachusetts 02114,[1] and Whitehead Institute for Biomedical Research[2] and Department of Biology, Massachusetts Institute of Technology,[3] Cambridge, Massachusetts 02142

Received 22 November 2000/Returned for modification 19 December 2000/Accepted 17 April 2001

In fat and muscle, insulin stimulates glucose uptake by rapidly mobilizing the GLUT4 glucose transporter from a specialized intracellular compartment to the plasma membrane. We describe a method to quantify the relative proportion of GLUT4 at the plasma membrane, using flow cytometry to measure a ratio of fluorescence intensities corresponding to the cell surface and total amounts of a tagged GLUT4 reporter in individual living cells. Using this assay, we demonstrate that both 3T3-L1 and CHO cells contain intracellular compartments from which GLUT4 is rapidly mobilized by insulin and that the initial magnitude and kinetics of redistribution to the plasma membrane are similar in these two cell types when they are cultured identically. Targeting of GLUT4 to a highly insulin-responsive compartment in CHO cells is modulated by culture conditions. In particular, we find that amino acids regulate distribution of GLUT4 to this kinetically defined compartment through a rapamycin-sensitive pathway. Amino acids also modulate the magnitude of insulin-stimulated translocation in 3T3-L1 adipocytes. Our results indicate a novel link between glucose and amino acid metabolism.

The GLUT4 glucose transporter is expressed predominantly in adipose and muscle tissues, where it accounts for the bulk of insulin-stimulated glucose uptake (12, 84, 95). In the presence of insulin, GLUT4 is redistributed from an intracellular compartment to the plasma membrane, where it facilitates the diffusion of glucose into the cell (15, 35, 73, 77, 102). Another glucose transporter isoform, GLUT1, is also expressed in fat and muscle tissues and is present at high levels in many other cell types and in cultured cell lines. A large proportion of GLUT1 is present on the plasma membrane even in the absence of insulin. Thus, while both GLUT1 and GLUT4 recycle at the plasma membrane, only GLUT4 recycling is characterized by significant intracellular sequestration, resulting from a slow rate of exocytosis, in the absence of insulin. Insulin increases the rate of GLUT4 exocytosis, with little or no decrease in its rate of endocytosis, so that in adipocytes the proportion of GLUT4 at the cell surface increases from <10% in the absence of insulin to 35 to 50% in its presence (41, 55, 85, 113, 114).

Characterization of the intracellular insulin-responsive GLUT4-containing compartment is complicated by the fact that GLUT4 resides in several morphologically distinct locations within the cell. Ultrastructural studies have shown that GLUT4 is present in tubulovesicular structures distinct from lysosomes, as well as in a perinuclear compartment that is in close vicinity to the trans-Golgi network (39, 96–98). Recent work demonstrates that approximately 40 to 45% of intracellular GLUT4 localizes in a transferrin receptor (TfnR)-positive endosomal compartment, while 50 to 60% is in a second, TfnR-negative compartment; it is GLUT4 in this TfnR-negative compartment that is rapidly mobilized upon insulin addition (1, 32, 46, 55, 57, 65, 76). In primary adipocytes, this TfnR-negative compartment can be subdivided into separate storage and exocytic pools of GLUT4 (55, 56). Other data suggest that the TfnR-positive GLUT4 compartment is the precursor of the TfnR-negative, insulin-responsive compartment (109). Moreover, targeting motifs within GLUT4 mediate its distribution between TfnR-negative and TfnR-positive compartments (66). Studies using the cation-dependent mannose 6-phosphate receptor (CD-M6PR) as an endosomal marker also find a similar, highly insulin-responsive, M6PR-negative pool of intracellular GLUT4 in 3T3-L1 adipocytes (64). Thus, it appears that GLUT4 is sequestered out of endosomes and into a highly insulin-responsive compartment. We have recently shown that 3T3-L1 adipocytes also possess an insulin-regulated secretory compartment containing ACRP30, a tumor necrosis factor alpha-like protein produced exclusively by adipocytes (7, 87, 92). This regulated secretory compartment is distinct from the insulin-regulated compartment containing GLUT4 (7).

Kinetic studies are consistent with the notion that there are multiple compartments through which GLUT4 traffics in adipocytes. GLUT4 recycles between the plasma membrane and intracellular sites in both basal and insulin-stimulated states, yet the initial externalization of GLUT4 after insulin addition is too rapid to be explained by the steady-state rate constants for exocytosis and endocytosis in the presence of insulin (14, 85, 113). It has therefore been argued that a two-pool model, with one intracellular and one plasma membrane compartment, does not explain the observed kinetics GLUT4 externalization after insulin addition and that GLUT4 must traffic through three or more compartments (37, 85, 114). Among these compartments is postulated to be a highly insulin-responsive intracellular compartment from which GLUT4 is rapidly mobilized by insulin (37, 56, 114). The GLUT4 accumulated in

* Corresponding author. Mailing address: Whitehead Institute for Biomedical Research, 9 Cambridge Center, Cambridge, MA 02142-1479. Phone: (617) 258-5216. Fax: (617) 258-6768. E-mail: lodish@wi.mit.edu.

this highly insulin-responsive compartment in the basal state is depleted upon insulin addition, and the steady-state exocytosis rate for GLUT4 in the continued presence of insulin becomes limited at some other step in the recycling pathway. This kinetically defined, highly insulin-responsive compartment in adipocytes corresponds well with the morphologically and biochemically defined, TfnR-negative compartments containing GLUT4 in adipocytes and myocytes, which are also depleted of GLUT4 after acute insulin stimulation (1, 32, 46, 55, 57, 65, 76).

The mechanisms controlling GLUT4 accumulation in this specialized insulin-sensitive compartment are poorly understood. The compartment is believed to be present only in muscle and fat and apparently develops early during 3T3-L1 adipocyte differentiation in cell culture (16, 19, 27, 34, 38, 39, 82, 89, 107). Some data indicate that a similar compartment to which GLUT4 is targeted is present in CHO cells, though this has been controversial (40, 44, 93, 105, 109). Kinetic studies suggest that even if some GLUT4 is targeted to a highly insulin-responsive compartment in CHO cells, sorting to this compartment is not efficient and does not constitute a major pathway by which GLUT4 traffics, in contrast to the case in adipocytes (3). Studies of the insulin-responsive aminopeptidase (IRAP), a protein of uncertain physiologic function that is thought to cotraffic with GLUT4, show that this protein participates in similar mechanisms for dynamic retention in the endosomal systems of CHO cells and 3T3-L1 adipocytes (43, 100). The assertion that the trafficking mechanisms employed by IRAP are identical those used by GLUT4 rests upon evidence that these proteins colocalize and cotraffic, with similar kinetics, under all conditions. Most data support this hypothesis (20, 23, 45, 62, 65, 81, 101). Of note, trafficking of IRAP, like that of GLUT4, is much more insulin-responsive in 3T3-L1 adipocytes than in CHO cells (43, 100). This is presumed to result from cell-type-specific differences, although, as with GLUT4, little is known about the mechanisms regulating IRAP accumulation and release from the highly insulin-responsive pool.

The present work began as a study of the cell type specificity of insulin-regulated GLUT4 trafficking. Using a novel reporter molecule to obtain detailed kinetic data, we find that GLUT4 participates in a highly insulin-responsive compartment not only in the fully differentiated 3T3-L1 adipocytes that we employ, but in undifferentiated 3T3-L1 preadipocytes as well. Such a compartment is not present in all cell types, since NIH 3T3 cells do not exhibit highly insulin-responsive trafficking. In CHO cells, we observe highly insulin-responsive trafficking only when the cells are cultured identically to 3T3-L1 adipocytes, in Dulbecco's modified Eagle's medium (DMEM). In standard F12 culture medium, the cells are less responsive. The highly insulin-responsive kinetics correlate with basal state redistribution of intracellular GLUT4 from the perinuclear region into punctate, peripheral structures. We pinpointed the amino acid content of these media as the relevant difference causing these trafficking characteristics: thus, given sufficient concentrations of essential amino acids, GLUT4 accumulates in a highly insulin-responsive compartment in CHO cells. Our data show that amino acids regulate GLUT4 accumulation in this compartment through a rapamycin-sensitive pathway. Finally, we demonstrate that amino acid sufficiency also modulates highly insulin-responsive GLUT4 trafficking in 3T3-L1 adipocytes and that this response is also rapamycin sensitive. Our data are consistent with the notion that both 3T3-L1 cells and CHO cells contain peripheral, highly insulin-responsive compartments through which GLUT4 traffics and that amino acid sufficiency modulates GLUT4 trafficking through these compartments in both cell types.

MATERIALS AND METHODS

Antibodies and reagents. Cell culture media and supplements were purchased from Life Technologies (Grand Island, N.Y.) and JRH Biosciences (Lenexa, Kans.). Anti-c-Myc monoclonal antibody (clone 9E10) was from Babco/Covance (Richmond, Calif.) and from Roche. An anti-insulin receptor β-chain antibody was purchased from BD Transduction Laboratories. Normal donkey serum and R-phycoerythrin (PE)-conjugated donkey $F(ab')_2$ anti-mouse immunoglobulin G (IgG) secondary antibody were purchased from Jackson Immunoresearch (West Grove, Pa.). Restriction enzymes were from New England Biolabs (Beverly, Mass.) and *Pfu* and *Taq* DNA polymerases were from Stratagene (La Jolla, Calif.). Wortmannin, LY294002, and rapamycin were from Calbiochem (La Jolla, Calif.). Oil red O and other chemicals were from Sigma (St. Louis, Mo.).

Cell culture. Murine 3T3-L1 fibroblasts were cultured in DMEM containing 10% fetal bovine serum (or 10% calf serum, where noted), and differentiation was induced according to established protocols (7, 22). Briefly, cells were allowed to reach confluence at least 2 days prior to the induction of differentiation. Differentiation was induced (on day 0) with medium containing 0.25 μM dexamethasone, 160 nM insulin, and 500 μM methylisobutylxanthine. After 48 h (day 2), the cells were fed with medium containing 160 nM insulin. After an additional 48 h (day 4), the cells were refed every 2 days with DMEM–10% fetal bovine serum. All media were supplemented with 2 mM glutamine, 100 U of penicillin per ml, and 0.1 mg of streptomycin per ml. Differentiation was monitored by noting the accumulation of lipid droplets, which typically began by day 4 of differentiation. Cells were considered fully differentiated between days 8 and 12. Throughout this report, the terms day 0 3T3-L1 cells and confluent 3T3-L1 preadipocytes are used interchangeably.

CHO-K1 cells stably expressing the murine ecotropic retrovirus receptor were kindly provided by David Hirsch, Roger Lawrence, and Monty Kreiger (Massachusetts Institute of Technology, Cambridge, Mass.) and maintained in Ham's F12 medium (F12) with 10% fetal bovine serum and 2 mM glutamine plus 100 U of penicillin and 0.1 mg of streptomycin per ml (5). NIH 3T3 cells were cultured in DMEM containing 10% calf serum, glutamine, penicillin, and streptomycin as above. Phoenix ecotropic retrovirus packaging cells were a gift from Garry Nolan (Stanford University Medical Center), and VE23 ecotropic retrovirus packaging cells were a gift from Merav Socolovsky (Whitehead Institute, Cambridge, Mass.) (51, 99, 103). Both retrovirus packaging cell lines were cultured in DMEM–10% fetal bovine serum with glutamine, penicillin, and streptomycin as above.

For experiments involving culture in minimal essential medium (MEM) with various amino acid concentrations, we used the MEM Select-Amine kit (Life Technologies). The 1× concentration of each amino acid was as follows (free base, in milligrams per liter): L-Arg, 102; L-Cys, 36; L-His, 30; L-Ile, 52; L-Leu, 52; L-Lys, 57; L-Met, 15; L-Phe, 32; L-Thr, 48; L-Trp, 10; L-Tyr, 35; and L-Val, 46. Relative to these concentrations, DMEM contains 2× Cys, Ile, Leu, Lys, Met, Phe, Thr, Tyr, and Val; 1.6× Trp; 1× His; and 0.67× Arg. F12 contains 1.67× Arg; 1.25× Cys; 0.5× His and Lys; 0.3× Met; 0.25× Leu, Thr, and Val; 0.2× Trp; 0.15× Phe and Tyr; and 0.08× Ile. All media contained 2 mM glutamine as well as penicillin and streptomycin as above.

Construction of a GLUT4 reporter. A human GLUT4 cDNA containing a c-Myc epitope tag in the first exofacial loop was kindly provided by Zhijun Luo and Joseph Avruch (Massachusetts General Hospital, Boston). This clone had been constructed as described by Kanai et al. (44). We fused the green fluorescent protein (GFP) coding sequence in frame to the carboxy terminus of this GLUT4 clone based on the results of Dobson et al. (18) that GLUT4-GFP appears to localize and traffic similarly to wild-type GLUT4. The GFP coding sequence from pEGFP-N1 (Stratagene) was first cloned into the pMX retroviral vector using *Eco*RI and *Not*I to generate plasmid pMX-GFP (68). PCR was done using primers 5′-GACATTTGACCAGATCTCGG-3′ and 5′-GGCCCGCGGG TCATTCTCATCTGGCCC-3′ to generate a ~110-bp *Bgl*II-*Sac*II fragment from the 3′ end of the rat GLUT4 cDNA (11). This PCR product and an *Eco*RI-*Bgl*II fragment containing most of the GLUT4*myc* cDNA were used in

a three-way ligation with *Eco*RI- and *Sac*II-digested pMX-GFP to generate pMX-GLUT4*myc*-GFP. Next, six additional *myc* epitope tags were added in tandem with the existing *myc* epitope tag, for a total of seven *myc* epitope tags. We first used PCR to amplify a ~240-bp *Eco*RI-*Hin*dIII fragment including the 5′ end of the rat GLUT4 cDNA and part of a *myc* tag, using primers 5′-CCG GCCGAATTCATGCCGTCGGGTTTCCAGCAGATC-3′ and 5′-CTTCAGA AATAAGCTTTTGCTCCTCTGCAGGACCCTGCCTACCCAGCCAAGTTG C-3′. This fragment was used to replace a corresponding fragment in pMX-GLUT4*myc*-GFP, creating a unique *Hin*dIII site within the *myc* epitope tag. A *Hin*dIII fragment containing six tandem *myc* epitope tags was amplified from plasmid pCS2+MT, a gift from Bill Schiemann (Whitehead Institute), using primers 5′-CCATCGATTTAAAGCTATGGAGCAAAAGCTTATTTCTGA AGAGG-3′ and 5′-CAGAAATAAGCTTTTGCTCCTCTGCAGGCTCAAGA GGTCTTGAGTTCAAGTCCTCTTC-3′. This fragment was inserted into the *Hin*dIII site of pMX-GLUT4*myc*-GFP, creating pMX-GLUT4*myc*7-GFP. The entire coding regions of the pMX-GLUT4*myc*-GFP and pMX-GLUT4*myc*7-GFP plasmids were verified by sequencing. The GLUT4*myc*7-GFP coding sequence was also placed in the pB retrovirus vector in order to optimize the potential translation efficiency; pB is identical to pMX except that two point mutations were introduced to eliminate potential start codons 5′ of the cloning site (J. S. Bogan, X. Liu, A. E. McKee, and H. F. Lodish, unpublished data). In this report, the GLUT4 reporter refers to that encoded by the GLUT4*myc*7-GFP sequence.

Production of retroviral supernatant and isolation of infected cell populations. Phoenix or VE23 ecotropic packaging cells were transfected with the pMX-GLUT4*myc*-GFP, pMX-GLUT4*myc*7-GFP, or pB-GLUT4*myc*7-GFP plasmid using calcium phosphate as described (51, 99, 103). In some instances, Phoenix cells were transfected using Fugene 6 (Roche) per the manufacturer's protocol. Media containing recombinant retroviruses were harvested 48 or 72 h after transfection and used to infect dividing 3T3-L1 preadipocytes, NIH 3T3 cells, or CHO cells expressing the murine ecotropic receptor. For 3T3-L1 preadipocytes infected with pMX-GLUT4*myc*7-GFP, flow cytometry demonstrated the presence of GFP in >90% of cells after infection. We isolated stable populations of infected cells expressing large, medium, and small amounts of the reporter by flow sorting cells falling within narrow ranges of GFP fluorescence. The sorted cells were expanded and differentiated into adipocytes, and insulin-stimulated GLUT4 trafficking (stimulated/basal) was measured by flow cytometry in all cases. We reasoned that there might be a trade-off between signal/noise (with small amounts of the reporter) and potential saturation of a trafficking mechanism (at large amounts of the reporter). In general, we chose medium- or high-expressing cells for use in subsequent experiments, since these had the greatest fold increase in cell surface GLUT4 after insulin treatment. These cells generally contained 5 to 10 times as much reporter protein as native GLUT4 in the mature 3T3-L1 adipocytes, as judged by immunoblotting with antibodies directed against the N and C termini of GLUT4 (kindly provided by Maureen Charron, Albert Einstein College of Medicine, Bronx, N.Y.). Similar optimization of reporter protein expression levels was carried out in NIH 3T3 and CHO cells.

Measurement of plasma membrane GLUT4 trafficking by flow cytometry. Confluent cells were reseeded on the indicated day of differentiation to six-well plates (Corning; Costar no. 3506) 1 day before use in experiments and starved in DMEM without fetal bovine serum for at least 3 h before insulin stimulation. Insulin was generally used at 160 nM; we occasionally used 80 or 200 nM and noted no difference between these concentrations in either 3T3-L1 or CHO cells. Insulin was added directly to the wells from a 100× stock. After treatment in the presence or absence of insulin for the times indicated in each figure, cells were quickly transferred to 4°C and washed with cold phosphate-buffered saline (PBS) containing 0.9 mM Ca^{2+} and 0.5 mM Mg^{2+} (PBS^{++}). All subsequent steps were carried out at 4°C, and staining of externalized *myc* epitope was done on adherent cells. Cells were incubated with a 1:200 dilution of anti-Myc (9E10) ascites or with purified 9E10 (25 μg/ml) in PBS^{++}–2% bovine serum albumin (BSA)–4% donkey serum for 1.5 h. Cells were then washed twice in PBS^{++} for 5 min each time. They were then incubated for 45 min in 12.5 to 25 μg of PE-conjugated donkey $F(ab')_2$ anti-mouse IgG secondary antibody per ml, diluted in PBS^{++}–2% BSA–4% donkey serum. Cells were rinsed twice in PBS^{++}, then washed three times in PBS^{++} for 10 min each, and resuspended by gentle scraping in PBS^{++}–2% BSA or PBS^{++}–5% fetal bovine serum for flow cytometry. For experiments involving insulin removal, cells were chilled as above after insulin stimulation and then washed twice with 5 mM sodium acetate–150 mM NaCl (pH 4.0) (48, 112). Cells were rewarmed in 37°C DMEM for the times indicated, restimulated with insulin or not restimulated, then returned to 4°C, and chilled with cold PBS^{++} before staining as above.

Flow cytometry was done on a FACScan or FACSCalibur cytometer (Becton Dickinson). Appropriate compensation between the FL1 and FL2 channels was set using uninfected (GFP negative) cells or cells stained with PE only (e.g., using a PE-conjugated anti-TfnR antibody [Pharmingen]). Pilot experiments demonstrated minimal loss of viability; only 2 to 3% of the cells typically stained with propidium iodide using the protocol described above, so propidium iodide was not used in experiments when accurate compensation and quantitation of fluorescence intensities was essential. For each sample, data from ≥10,000 cells were collected. We used median fluorescence intensities for quantification, since this measure of central tendency is least sensitive to outliers. For each sample, the PE and GFP fluorescences specifically attributable to the presence of the GLUT4 reporter were determined by subtracting background fluorescences, measured using control unstained cells and cells not expressing the reporter, respectively. These control cells were treated with the same conditions (e.g., type of serum and medium and amino acid concentrations) used for the experimental cells. The ratio of fluorescence intensities plotted on the vertical axes of many figures is a relative, not absolute, measure of the proportion of GLUT4 at the cell surface. The scales are numbered arbitrarily and are not intended to permit comparison in absolute terms of data obtained in different experiments. In some of the kinetic studies (Fig. 7 to 10), the data were subjected to a simple smoothing operation. This consisted of calculating an equation, $0.25\ r_{t-1} + 0.5\ r_t + 0.25\ r_{t+1}$, where r is the ratio of specific fluorescences for time point t. This calculated value was used for time points $t = 2$ to $t = n - 1$, where n is the total number of time points. For the last time point, $t = n$, $0.33\ r_{t-1} + 0.67\ r_t$ was calculated. Basal values of r (r_1) were unchanged.

Subcellular fractionation. Four 10-cm plates of 3T3-L1 adipocytes were used per condition to isolate low-density microsomal and plasma membrane fractions (Fig. 1b). Eight and ten plates per condition were used to isolate low-density microsomes for analysis by sucrose density gradient centrifugation (Fig. 1c) and in vesicle immunopurification experiments (Fig. 1d), respectively. Five plates of adipocytes and 10 plates of preadipocytes were used per condition in the experiments presented in Fig. 3b and 4b, respectively. For experiments presented in Fig. 1b and 1c, cells were serum starved overnight, treated in the presence or absence of insulin (160 nM, 10 min), then transferred to 4°C, and washed with cold PBS^{++}. For the vesicle immunopurification (Fig. 1d), cells were starved overnight, then transferred to 4°C, and washed with cold PBS^{++} without insulin stimulation. For kinetic studies (Fig. 3b and 4b), 480 nM insulin was used (added from a prewarmed 3× stock) in order to maximally and simultaneously stimulate all of the cells on each 10-cm dish. Cell were transferred to 4°C and washed with cold PBS^{++} at the indicated times. In all cases, cells were next washed once with cold 250 mM sucrose–10 mM Tris (pH 7.4)–0.5 mM EDTA (buffer A). Cells were resuspended by scraping in cold buffer A with Complete protease inhibitors (Roche) and then homogenized using 16 strokes (four plates) or 25 strokes (eight plates) in a Dounce-type Teflon tissue grinder (Kontes no. 22; VWR). All subsequent steps were performed at 4°C. The homogenate was centrifuged at 11,500 rpm in an SS-34 rotor (16,000 × *g*) for 20 min. The pellet was resuspended in buffer A and then layered on top of 1.12 M sucrose–10 mM Tris (pH 7.4)–0.5 mM EDTA in a ~2-ml centrifuge tube. The samples were centrifuged in a TLS-55 rotor at 36,000 rpm (158,000 × *g*) for 20 min. The interface was removed using a syringe, diluted in buffer A, and centrifuged in a TLA-100.2 rotor at 37,000 rpm (74,000 × *g*) for 9 min. The pellet was resuspended in buffer A and centrifuged again under identical conditions. The pellet from this centrifugation, designated PM, was resuspended in TNET (1% Triton X-100, 150 mM NaCl, 20 mM Tris [pH 8.0], 2 mM EDTA) or in radioimmunoprecipitation assay (RIPA) buffer (PBS, 1% NP-40, 0.5% sodium deoxycholate, 0.1% sodium dodecyl sulfate [SDS]) and stored at −20°C until needed.

The supernatant from the initial centrifugation was recentrifuged at 19,000 rpm in an SS-34 rotor (43,000 × *g*) for 30 min. The pellet (designated HDM) was resuspended in TNET or RIPA buffer and stored at −20°C. The supernatant was centrifuged at 65,000 rpm in a Ti70.1 rotor (39,000 × *g*) for 75 min. The pellets from this centrifugation, designated LDM, were resuspended in either TNET or RIPA buffer and stored at −20°C until needed or resuspended in 500 μl of 50 mM sucrose–10 mM Tris (pH 7.4)–0.5 mM EDTA and loaded on top of a 4.9-ml 10 to 30% (wt/vol) linear sucrose gradient prepared in 10 mM Tris (pH 7.4)–0.5 mM EDTA. Separation of low-density microsomes by sedimentation was done essentially as described with minor modifications (19). The samples were centrifuged in an SW50.1 rotor at 48,000 rpm (280,000 × *g*) for 55 min. Fractions were collected from the tops of the gradients. Equal volumes of each fraction were analyzed by SDS-polyacrylamide gel electrophoresis (PAGE) and immunoblotting, and the total protein content in each fraction was determined using the Micro-BCA kit (Pierce). In experiments where LDM and PM fractions were analyzed directly (without sedimentation of the LDM), total protein content was first determined and then equal amounts of protein were analyzed by SDS-PAGE and immunoblotting.

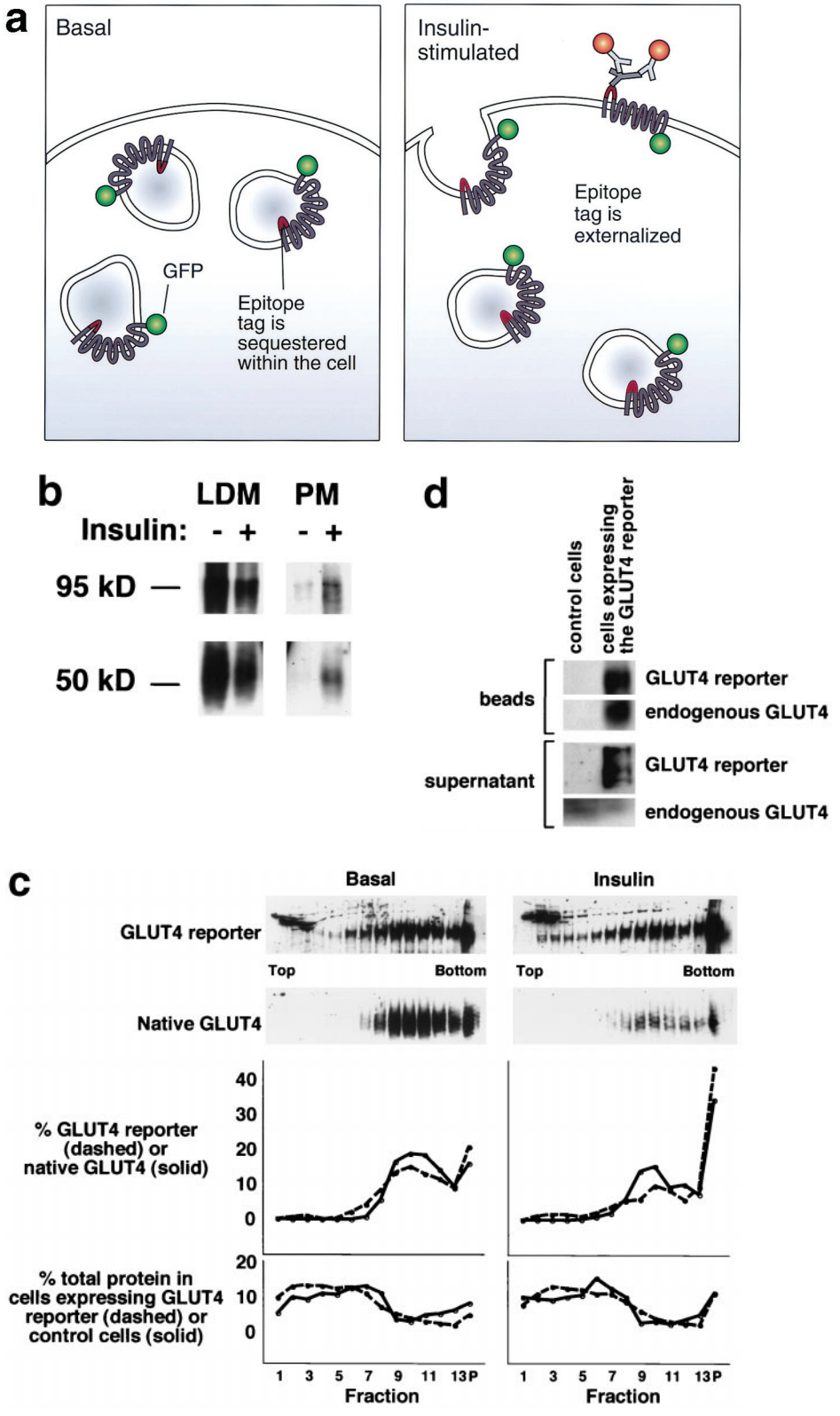

FIG. 1. Assay for changes in proportion of GLUT4 at the plasma membrane. A GLUT4 reporter containing Myc epitope tags in the first exofacial loop as well as GFP fused in frame at the carboxy terminus was constructed as described in Materials and Methods. As shown in panel a, this reporter enables measurement of changes in the proportion of GLUT4 at the plasma membrane as changes in the ratio of fluorescence intensities corresponding to cell surface and total amounts of the reporter. Cell surface GLUT4 reporter is detected using an anti-Myc primary antibody and PE-conjugated secondary antibody. Total GLUT4 reporter is proportional to GFP fluorescence. (b) Low-density microsome (LDM) and plasma membrane (PM) fractions were isolated from 3T3-L1 adipocytes expressing the reporter and analyzed by SDS-PAGE and immunoblotting. Equal amounts of protein were loaded in each lane. Immunoblotting was done using an antibody directed against the carboxyl terminus of GLUT4 and demonstrates that both the reporter (95 kDa) and native GLUT4 (50 kDa) are redistributed from the LDM fraction to the PM after acute insulin treatment. The amount of translocation is quantitatively similar. (c) The LDM fractions from basal and insulin-stimulated

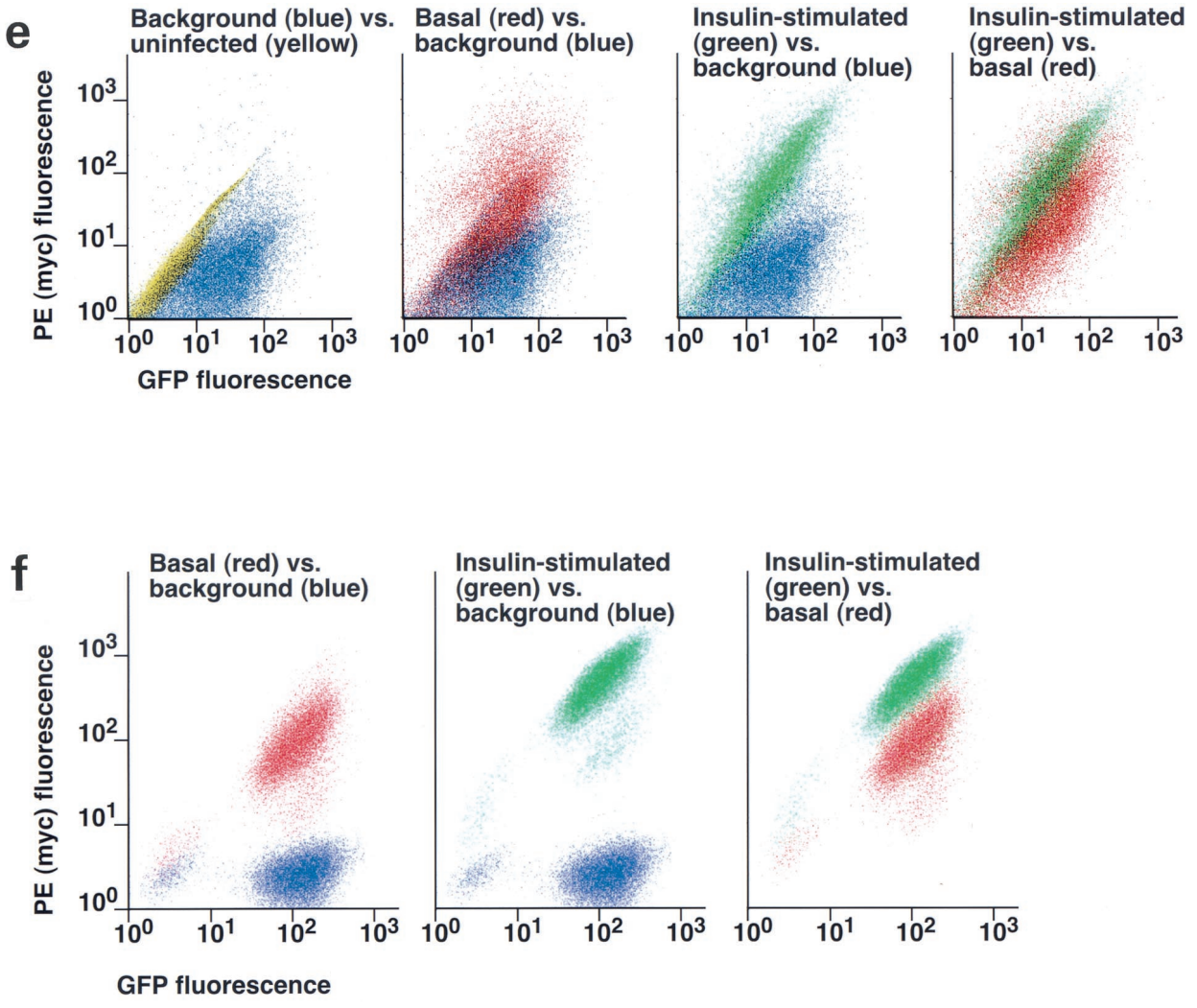

3T3-L1 adipocytes expressing the reporter and from control cells were further separated by sedimentation on a 10 to 30% linear sucrose gradient, as described in Materials and Methods. Equal volumes of each gradient fraction were analyzed by to determine total protein and by SDS-PAGE and immunoblotting to detect native GLUT4 (in control cells, using an anti-GLUT4 antibody) and the GLUT4 reporter (using an anti-Myc antibody). As shown in the top panels, the reporter and endogenous GLUT4 cosediment in both basal (left) and insulin-stimulated (right) cells. Densitometry was used to quantify the bands (middle panels), and data are plotted as the percentage of the total reporter or native GLUT4 present in each gradient fraction; these profiles are quite similar. As a control, the percentage of total protein present in each gradient fraction is plotted (lower panels); these profiles are similar to each other and distinct from those of the GLUT4 reporter and endogenous GLUT4. (d) LDM fractions from unstimulated 3T3-L1 adipocytes expressing the reporter and from control cells not expressing the reporter were used in vesicle immunopurification experiments. LDM fractions were incubated with two pooled anti-GFP monoclonal antibodies, followed by protein G-Sepharose beads. After pelleting and washing of the beads, the immunopurified material was eluted in sample buffer and analyzed by SDS-PAGE and immunoblotting with an anti-GLUT4 rabbit polyclonal antibody. As shown in the upper two panels, native GLUT4 is detected in the immunopurified material. The lower panels present a similar immunoblot of the supernatants and demonstrate that even though the immunopurification did not quantitatively remove all of the GLUT4 reporter, the endogenous GLUT4 is depleted, as expected. (e) Flow cytometry is used to quantify the insulin-stimulated change in the proportion of GLUT4 at the plasma membrane of 3T3-L1 adipocytes expressing the reporter protein. Serum-starved cells were treated or not with insulin, chilled, stained for externalized Myc epitope tag, and analyzed by FACS as described in Materials and Methods. PE and GFP fluorescence intensities are plotted on the vertical and horizontal axes, respectively, of the dotplots presented. Note that both scales are logarithmic. Compared to the background fluorescence of cells not expressing the reporter (yellow), cells expressing the reporter (blue) have increased GFP fluorescence (leftmost panel). Among cells expressing the reporter, unstained cells (blue) and basal (stained for cell surface Myc, shown in red) and insulin-stimulated (stained for cell surface Myc, shown in green) populations have progressively increasing PE fluorescence with no change in GFP fluorescence. Control experiments show that the background staining is negligible (not shown). The four panels allow direct comparison of pairs of samples. In this experiment, insulin caused a fourfold increase in the ratio of median fluorescence intensities attributable to externalized Myc epitope and to GFP expression, corresponding to a fourfold increase in the proportion of total GLUT4 present at the cell surface. (f) Flow cytometry was used to measure insulin-stimulated GLUT4 translocation in confluent CHO cells. As in panel e, PE fluorescence (proportional to cell surface GLUT4 reporter) is plotted on the vertical axis and GFP fluorescence (proportional to total GLUT4 reporter) is plotted on the horizontal axis; both scales are logarithmic. Background (unstained) cells expressing the reporter are shown in blue, and basal and insulin-stimulated populations are shown in red and green, respectively. The three panels allow direct comparison between each pair of samples. There is a minor population of unstained cells (blue) within the first decade of each scale; these cells do not express the GLUT4 reporter and conveniently demonstrate that the flow cytometer is properly adjusted to compensate for fluorophore bleedthrough. Compared to 3T3-L1 adipocytes, the background fluorescences (both PE and GFP) account for much less of the total fluorescence intensities in CHO cells, and the signal-noise ratio is correspondingly increased (compare panels e and f). In this experiment, insulin stimulated a 3.5-fold increase in the proportion of total GLUT4 present at the cell surface.

For vesicle immunopurification experiments, LDM fractions were resuspended in PBS^{++}–2% BSA and then incubated overnight at 4°C in the presence of 25 μl (10 μg) of anti-GFP monoclonal antibodies (Roche). Protein G-Sepharose beads were preblocked with PBS^{++}–2% BSA, then added to each sample, and incubated for 1 h at 4°C. The beads were pelleted, and the supernatant was transferred to new tubes and frozen until needed. The beads were washed five times in PBS^{++}–2% BSA and then three times more in PBS^{++} without BSA. Material was eluted from the beads at 65°C for 30 min in SDS-PAGE sample buffer, and equal volumes were loaded for electrophoresis and subsequent immunoblotting.

Other methods. Immunofluorescence microscopy of permeablized cells was done essentially as described (7). Cells were fixed with 4% paraformaldehyde in PBS for 40 min, permeablized with 0.2% Triton X-100 for 5 min, and then washed extensively with PBS^{++}. Staining of CHO cells expressing the GLUT4 reporter was done in order to increase the fluorescent signal from that due to GFP alone and employed a monoclonal anti-Myc antibody and a fluorescein isothiocyanate (FITC)-conjugated secondary antibody.

For immunofluorescence microscopy of unpermeablized cells (Fig. 6a), cells on coverslips were stimulated with insulin, then transferred to 4°C, and washed with cold PBS^{++}. Living cells were stained at 4°C using anti-Myc (9E10) monoclonal antibody (25 μg/ml) in PBS^{++}–2% BSA–4% goat serum. After 1 h at 4°C, cells were washed and incubated with Alexa594-conjugated goat anti-mouse IgG secondary antibody (10 μg/ml) (Molecular Probes). Cells were then fixed with parafomaldehyde as described above, and coverslips were mounted using Prolong antifade reagent (Molecular Probes). Microscopy was done using a Zeiss Axiophot microscope, and images were acquired on film. In order to compare fluorescence intensity due to externalized Myc epitope, GFP images were acquired first using an exposure time calculated by the camera, and the exposure time used for the corresponding Alexa594 images was set as a constant fraction of the GFP exposure time. In this way, we attempted to normalize the images of externalized Myc epitope tag for variations in the total amount of the reporter protein and cell density.

Oil red O staining was done on cells grown in 10-cm dishes. Cells were fixed with 4% paraformaldehyde for 45 min at room temperature, permeablized with 0.2% Triton X-100 for 5 min at 4°C., and stained using a 2-mg/ml solution of Oil red O in ethanol (24). Phase-contrast and bright-field microscopy was done using an Olympus inverted microscope.

RESULTS

Novel assay for GLUT4 trafficking at the plasma membrane. To assay changes in the proportion of GLUT4 that is present at the plasma membrane, we constructed a cDNA encoding a GLUT4 reporter protein. This protein contains seven c-Myc epitope tags in the first exofacial loop of GLUT4 and GFP fused in-frame at the carboxy terminus. As shown in Fig. 1a, expression of this protein in cells enables us to measure changes in the proportion of GLUT4 at the cell surface as changes in a ratio of fluorescence intensities. We use an anti-Myc monoclonal antibody followed by a PE-conjugated secondary antibody to detect reporter protein present at the surface of living cells. Green (GFP) fluorescence indicates the total amount of the reporter present in each cell. Thus, the ratio of PE to GFP fluorescence intensities corresponds to the proportion of total GLUT4 that is present at the plasma membrane. We employ flow cytometry to measure these fluorescence intensities simultaneously and on a cell-by-cell basis.

We placed the GLUT4 reporter in a murine retrovirus vector and infected 3T3-L1 preadipocytes. Using fluorescence-activated cell sorting (FACS), we isolated a population of cells falling within a narrow range of GFP fluorescence intensities; individual cells in this population express similar amounts of the reporter protein. These 3T3-L1 cells underwent normal adipose cell differentiation (see below), and we took several approaches to confirm that the GLUT4 reporter traffics appropriately. We first used differential centrifugation to isolate low-density microsomal (LDM) and plasma membrane (PM) fractions from cells expressing the GLUT4*myc*7-GFP reporter and from control cells. As shown in Fig. 1b, acute insulin treatment causes similar decreases in the amounts of both native GLUT4 (~50 kDa) and the reporter protein (~95 kDa) in the LDM fraction. Correspondingly, insulin treatment causes similar increases in both proteins in the PM fraction. Of note, the increases in the plasma membrane fraction are in the 5- to 10-fold range (insulin/basal), as judged by densitometry of several experiments. Thus, both the reporter and endogenous GLUT4 proteins redistribute to the plasma membrane in a quantitatively similar manner.

Figure 1c presents data further substantiating that the GLUT4 reporter codistributes with endogenous GLUT4 in low-density microsomes prepared from 3T3-L1 adipocytes. In this experiment, we first isolated LDM fractions from basal and insulin-stimulated cells containing the reporter and from control cells not expressing the reporter. We layered these fractions on top of 10 to 30% linear sucrose density gradients and sedimented the microsomes by centrifugation. We then collected fractions from each sample and immunoblotted to detect endogenous GLUT4 or the reporter. As shown in the upper left panels of Fig. 1c, both native GLUT4 and the reporter sediment similarly in unstimulated cells, with the bulk of both proteins present in fractions 8 to 13 and in the pellet (middle left panel). In insulin-stimulated cells, the distributions of both endogenous GLUT4 and the reporter shift to the pellet; fractions 8 to 13 contain most of the remaining protein, as in the unstimulated cells (top and middle right panels). As a control, total protein was measured in each fraction and is plotted at the bottom of the figure for unstimulated cells (left) and for insulin-stimulated cells (right). These profiles are similar for cells containing the GLUT4 reporter and for control cells and are distinct from the distributions of endogenous GLUT4 and the GLUT4 reporter. The distribution of the GLUT4 reporter on these gradients is broader than that of native GLUT4, perhaps because the reporter is expressed at roughly fivefold-higher levels (not shown) and may be present in a more heterogeneous population of vesicles. Nonetheless, the bulk of GLUT4 reporter in low-density microsomes is present in vesicles that sediment similarly to those containing native GLUT4 in both basal and insulin-stimulated cells.

To further determine if endogenous GLUT4 and the GLUT4 reporter are present in the same vesicles, we used an anti-GFP antibody and protein G-Sepharose beads to immunopurify vesicles from the LDM fraction of unstimulated 3T3-L1 adipocytes expressing the reporter. As shown in Fig. 1d, immunoblotting demonstrates the presence of endogenous GLUT4 in these vesicles, as well as confirming the presence of the reporter. As a control, 3T3-L1 adipocytes not expressing the GLUT4 reporter were treated in parallel; in this case, neither the GLUT4 reporter nor endogenous GLUT4 is detected in the material eluted from the beads. Endogenous GLUT4 is detected in the supernatants from both samples and, as expected, is depleted from that of the cells expressing the reporter. Some GLUT4 reporter also remains in the supernatant, and we estimate that the immunopurification removed

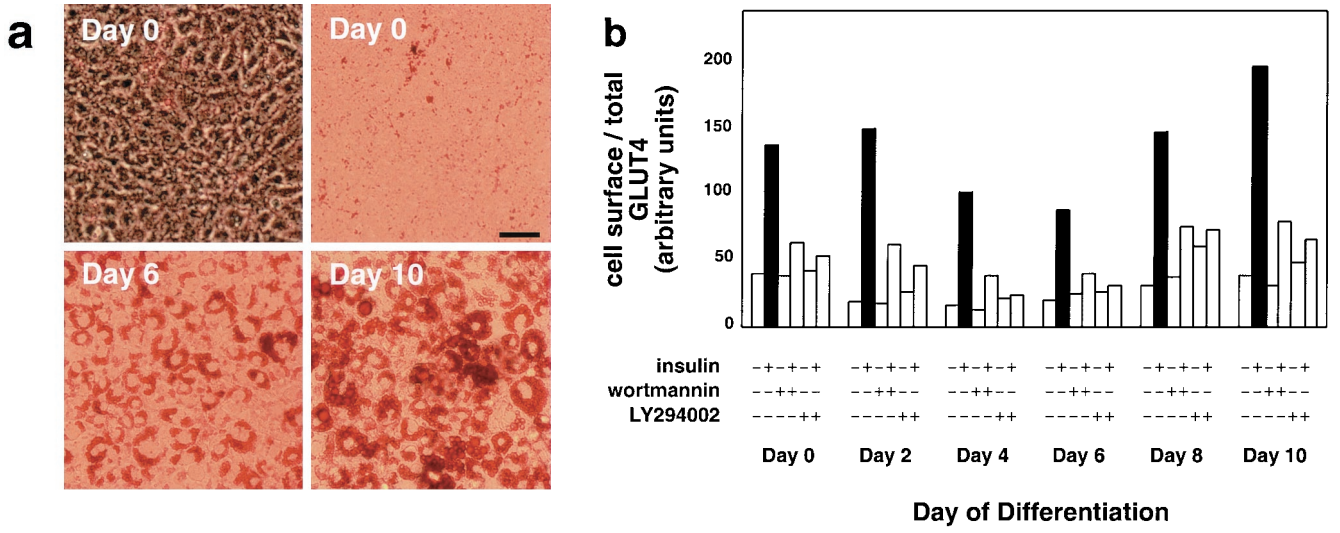

FIG. 2. Adipose differentiation and GLUT4 translocation in 3T3-L1 cells. 3T3-L1 preadipocytes were infected with a retrovirus containing the GLUT4 reporter, and flow sorting was used to isolate a population of cells falling within a narrow range of GFP fluorescence intensities. These cells were expanded and used in experiments; because the retrovirus integrates into the genome, the population is stable. These cells undergo normal 3T3-L1 adipose differentiation, as demonstrated by staining lipid with Oil red O. (a) Phase-contrast (upper left) and bright-field (upper right and lower left and right) microscopy of cells at the indicated days of differentiation is shown. Scale bar, 50 μm. (b) Confluent 3T3-L1 preadipocytes (day 0) or 3T3-L1 cells that had undergone differentiation for various lengths of time were stimulated or not with insulin (160 nM, 10 min), and changes in the proportion of GLUT4 reporter present at the cell surface were measured using flow cytometry as described in the text. Some samples were treated with either 100 nM wortmannin (42) or 50 μM LY294002 (8, 13) for 40 min prior to insulin addition, as noted. The amount of the reporter within each cell varies during 3T3-L1 differentiation and is increased approximately threefold on days 2 and 4 (not shown). We attribute this to increased activity of the retroviral promoter as the cells undergo clonal expansion at the onset of adipocyte differentiation, especially since we also observed increased expression of the reporter in preconfluent, dividing cells (91). Because the assay measures changes in the ratio of cell surface to total GLUT4 rather than in the absolute amount of cell surface GLUT4, the data presented are internally controlled for this variation, and data from different days of differentiation can be meaningfully compared. The numbering on the vertical scale indicates a relative measure of GLUT4 at the cell surface, and these arbitrary units cannot be compared in absolute terms to those in other figures. In all instances, insulin stimulates GLUT4 exocytosis, and this effect is blocked by either of the two phosphatidylinositol-3-kinase inhibitors.

only 50 to 75% of vesicles containing the reporter protein from the starting microsomes. The results indicate that endogenous GLUT4 and the GLUT4 reporter are present together in a population of vesicles within the low-density microsomal fraction.

To measure insulin-stimulated GLUT4 externalization in differentiated 3T3-L1 adipocytes expressing the reporter, we used flow cytometry as shown in Fig. 1e. This technique allows simultaneous measurement of PE fluorescence (corresponding to cell surface GLUT4 reporter and shown on the vertical scale) and GFP fluorescence (corresponding to total GLUT4 reporter and shown on the horizontal scale). Control 3T3-L1 adipocytes not expressing the reporter (shown in yellow) have background fluorescences that are highly correlated across the relevant wavelengths and appear as a diagonal population. For cells expressing the reporter but not stained for cell surface Myc epitope (shown in blue), fluorescence along the PE axis is due entirely to this background autofluorescence. Control experiments using secondary antibody without primary (anti-Myc) antibody, as well as control experiments using both primary and secondary antibodies on cells not expressing the reporter, demonstrate that background staining is negligible (data not shown); thus, essentially all of the increase in PE fluorescence observed in the basal (red) and insulin-stimulated (green) populations is due to detection of Myc on the cell surface. Similarly, the GFP fluorescence attributable to the GLUT4 reporter can be determined by subtracting the background autofluorescence (yellow). Within each population of stained cells (basal and insulin stimulated), the amount of staining for cell surface Myc correlates with the amount of the reporter present and therefore with GFP fluorescence. The populations therefore lie along a diagonal, and GLUT4 exocytosis results in a net translocation of the entire population upwards, along the PE axis, with no change in the slope of the diagonal. Within this defined population of cells we observe no saturation of the recycling mechanism: changes in the proportion of GLUT4 at the cell surface are equivalent, even among cells expressing ~50-fold-different amounts of the reporter.

To measure GLUT4 trafficking at the surface of CHO cells, we infected CHO cells expressing the murine ecotropic retrovirus receptor with a retrovirus carrying the GLUT4 reporter and used FACS to isolate cells falling within a narrow range of GFP fluorescence intensities. Upon insulin stimulation of these cells, we again noted externalization of the GLUT4 reporter, as detected by flow cytometry. As shown in Fig. 1f, autofluorescence accounts for much less of the total fluorescent signals in CHO compared to 3T3-L1. Thus, the unstained cells expressing the reporter do not fall along a diagonal because autofluorescence contributes minimally. Similarly, whereas autofluorescence contributes perhaps one-quarter of the total PE fluorescence in 3T3-L1 adipocytes, in CHO cells this

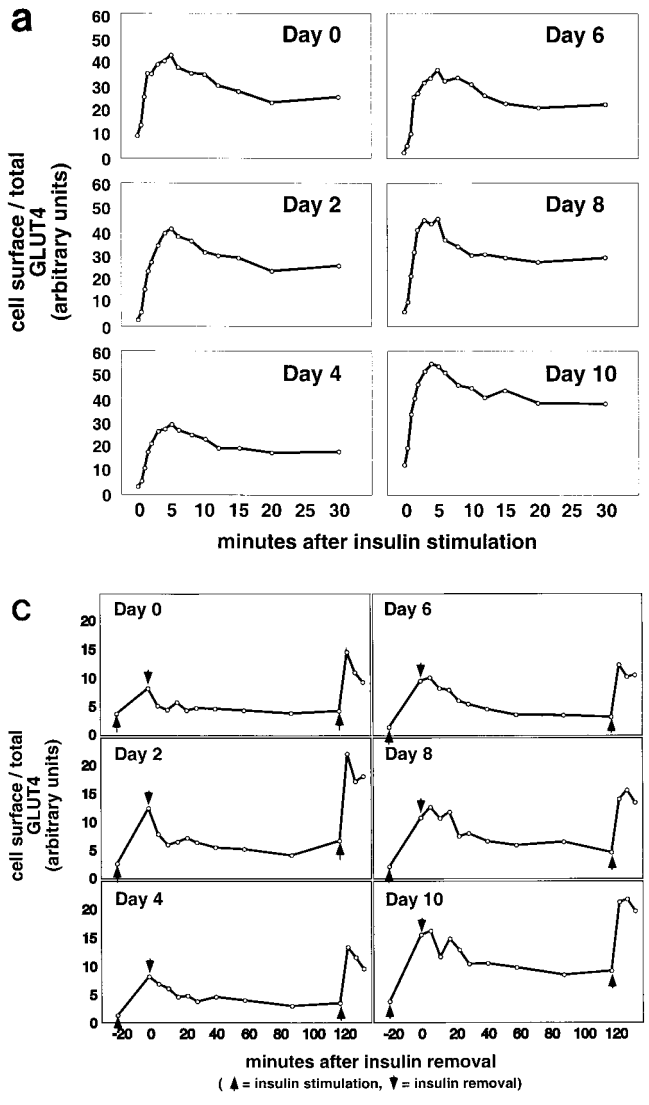

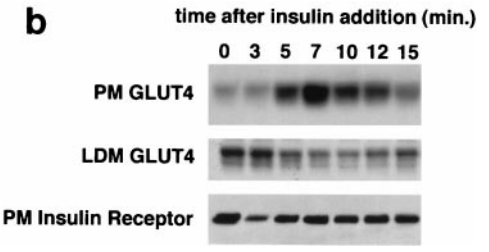

FIG. 3. Kinetics of GLUT4 trafficking in 3T3-L1 cells. (a) Confluent 3T3-L1 preadipocytes (day 0) or 3T3-L1 cells at various stages of adipocyte differentiation (as indicated) were treated with insulin for various lengths of time, and changes in the proportion of GLUT4 reporter present at the cell surface were analyzed. Data are plotted for basal cells and for cells treated with 80 nM insulin for 0.5, 1, 1.5, 2, 3, 4, 5, 6, 8, 10, 12, 15, 20, or 30 min. Membrane trafficking was stopped by washing with cold PBS, cells were stained at 4°C for externalized Myc epitope tag using a PE-conjugated secondary antibody, and PE and GFP fluorescence intensities were measured using flow cytometry as described in the text. Regardless of the state of differentiation, insulin causes a rapid externalization of GLUT4 that peaks 4 to 5 min after insulin addition. Subsequently, there is a net internalization, so that a steady state in the presence of insulin is reached 20 min after insulin addition. The numbering on the vertical scale indicates a relative measure of GLUT4 at the cell surface, and these arbitrary units cannot be compared in absolute terms to those in other figures. (b) Insulin-stimulated translocation of endogenous GLUT4 to the plasma membrane of 3T3-L1 adipocytes was analyzed by subcellular fractionation. Cells were starved overnight and then stimulated with 480 nM insulin (added from a prewarmed, 3× stock) for various amounts of time. Cells were transferred to 4°C, washed with cold PBS, and fractionated as described in Materials and Methods. Plasma membrane (PM) and low-density microsomal (LDM) fractions were analyzed by immunoblotting. Equal amounts of protein were loaded in each lane. GLUT4 translocates to the plasma membrane in a biphasic pattern, with a peak at 7 min after insulin addition, followed by a subsequent decrease. A reciprocal pattern is observed in the LDM fraction. As a control, the PM immunoblot was reprobed with an anti-insulin receptor (β-subunit) antibody, which demonstrates similar amounts of insulin receptor at the plasma membrane at all time points. The experiment was performed twice, with similar results each time. (c) 3T3-L1 preadipocytes (day 0) or cells at various times during adipocyte differentiation were stimulated with 80 nM insulin for 20 min, then placed at 4°C, and washed with an acidic buffer to remove insulin. Cells were rewarmed in serum-free medium to allow GLUT4 reinternalization for 6, 12, 18, 24, 30, 40, 60, 90, or 120 min; some cells that had been rewarmed for 120 min were restimulated with 80 nM insulin for 5, 10, or 15 min. Cells were stained for cell surface Myc epitope and analyzed by flow cytometry as described in the text. In all instances, the GLUT4 reporter was reinternalized after removal of insulin and recycles upon readdition of insulin.

figure is reduced to 1 to 2%. As with 3T3-L1 adipocytes, the distribution of each of the stained populations (basal and insulin stimulated, shown in red and green, respectively) falls along a diagonal because the amount of Myc epitope at the surface of each cell is proportional to the amount of the reporter present within that cell. Insulin stimulates the entire population to shift upward (~4-fold) along the PE (Myc) axis, with no change in the slope of the diagonal, consistent with exocytosis of the GLUT4 reporter equally and with no saturation of the recycling mechanism among the infected cells.

Insulin stimulates GLUT4 translocation similarly in undifferentiated 3T3-L1 cells and throughout 3T3-L1 adipose differentiation. One difficulty in working with 3T3-L1 cells is that if the undifferentiated fibroblasts are allowed to become confluent, they must be induced to undergo adipose differentiation or they will lose that capacity. This characteristic makes the introduction of exogenous proteins by stable transfection technically difficult, since the cells invariably become confluent during clonal selection. We circumvented this difficulty by isolating a pool of cells infected with a replication-deficient retrovirus encoding the reporter protein. Over 90% of the target 3T3-L1 fibroblasts were infected, and those falling within a narrow window of GFP fluorescence were isolated by FACS; individual cells in this sorted population express similar amounts of the reporter. Figure 2a demonstrates that these sorted cells undergo normal 3T3-L1 adipose differentiation, as assessed by Oil red O staining to highlight the development of intracellular lipid droplets.

We next sought to determine when during the course of 3T3-L1 adipocyte differentiation the cells become competent to translocate GLUT4 to the plasma membrane after insulin addition. Cells expressing the reporter were differentiated to different days, and the ability of insulin to stimulate GLUT4

exocytosis was tested as described above. Unexpectedly, and as shown in Fig. 2b (and subsequently in Fig. 3a), we found that insulin stimulates GLUT4 exocytosis at all times during 3T3-L1 differentiation, even in undifferentiated, confluent fibroblasts. Moreover, as shown in Fig. 2b, insulin-triggered GLUT4 exocytosis is invariably blocked by treatment of the cells with phosphatidylinositol-3-kinase inhibitors, either wortmannin or LY294002. In several experiments we noted that the overall fold increase in cell surface GLUT4 was greater at day 2 of differentiation than at day 0, primarily due to more pronounced intracellular sequestration in unstimulated cells; nonetheless, the effect at day 0 is robust and consistently observed (Fig. 2b and see below).

To determine if the kinetics of insulin-stimulated GLUT4 externalization vary during the course of 3T3-L1 differentiation, we stimulated cells at different days of differentiation and assayed changes in the proportion of GLUT4 at the cell surface as a function of time. As shown in Fig. 3a, insulin triggers a rapid redistribution of GLUT4 to the cell surface, with identical kinetics at all days of 3T3-L1 differentiation. In all cases there was a biphasic response to insulin addition, with an initial rapid externalization of GLUT4 such that the greatest proportion was present on the plasma membrane 4 to 5 min after insulin addition. Subsequently, in all cases, the fraction of GLUT4 on the plasma membrane fell by 20 to 40% and reached a steady state by 15 to 20 min after insulin addition. This overshoot of the steady-state proportion of GLUT4 at the cell surface in the presence of insulin presumably corresponds to rapid mobilization (and depletion) of GLUT4 in a highly insulin-sensitive compartment, as noted in the introduction.

Because of the relative ease with which we are able to measure GLUT4 at the cell surface, all of the data points presented in all six panels of Fig. 3a were acquired in the same experiment. As noted above, our assay is internally controlled for the amount of reporter present within each cell. Thus, any data point in any of the six panels can be directly compared to any other data point in the figure. Clearly, unstimulated day 2 cells have a lower proportion of GLUT4 on the cell surface than unstimulated confluent fibroblasts (day 0 cells), in agreement with the data presented in Fig. 2b. While the slightly higher basal level of GLUT4 at the surface of confluent fibroblasts lessens the overall fold increase in cell surface GLUT4 after insulin addition, the overall picture is similar in undifferentiated 3T3-L1 cells and in cells that have undergone any degree of adipose differentiation. Importantly, the overshoot of the final, steady-state response in the presence of insulin is present in all cases.

To determine if insulin stimulates externalization of native GLUT4 with a similar overshoot of the final steady-state response, we performed subcellular fractionation of 3T3-L1 adipocytes. These cells do not express the GLUT4 reporter protein, and we detected endogenous GLUT4 by immunoblotting equal amounts of total protein from each time point. As shown in Fig. 3b, we observed a rapid accumulation of GLUT4 in the plasma membrane fraction (PM GLUT4) and a corresponding decrease in GLUT4 present in the low-density microsomal fraction (LDM GLUT4). The presence of GLUT4 in the PM fraction peaks at 7 min after insulin addition; subsequently, there is a decrease in the amount present. Similarly, GLUT4 in the LDM fraction is first depleted and subsequently reaccumulates slightly. As a control, we reprobed the blot of the plasma membrane fractions with an anti-insulin receptor β-chain antibody. As shown in the lower panel of the figure, this detected similar amounts of insulin receptor at the plasma membrane at most time points. There is a slight decrease immediately (3 min) after insulin addition, perhaps due to internalization of the receptor, and the amount normalizes at subsequent times. Thus, immunoblotting of subcellular fractions demonstrates that native GLUT4 traffics with kinetics similar to those we observed using the tagged GLUT4 reporter and the FACS-based assay.

We next examined reinternalization and recycling of the GLUT4 reporter after insulin removal. Based on the results shown in Fig. 3a, cells were stimulated with insulin for 20 min so that the redistribution of GLUT4 to the plasma membrane would be at steady state, then chilled, washed with a low-pH buffer to remove insulin, and rewarmed in serum-free medium for various amounts of time. Cells were allowed to reinternalize GLUT4 for up to 2 h, at which time they were restimulated with insulin for 5, 10, or 15 min. As shown in Fig. 3c, the reporter protein is reinternalized in undifferentiated 3T3-L1 cells and at all times of 3T3-L1 adipocyte differentiation and is recycled upon restimulation with insulin in all cases. As in Fig. 3a, all of the data points in Fig. 3c were collected in parallel and can be compared, even if presented in different panels of the figure. The rate of reinternalization is slightly prolonged in more differentiated cells compared to less differentiated cells. Finally, restimulation with insulin causes reexternalization of the reporter; the magnitude and kinetics of this effect are similar to the initial response, and the biphasic pattern described above is likely present. We conclude that the addition of Myc epitope tags and fusion of GFP to the carboxy terminus of GLUT4 do not impair its ability to undergo endocytosis or insulin-stimulated recycling at the plasma membrane.

As noted above, we were surprised to observe insulin-stimulated GLUT4 translocation to the plasma membrane of undifferentiated 3T3-L1 preadipocytes. To determine if this response is general to other cell types, we expressed the GLUT4 reporter protein in NIH 3T3 cells by retrovirus infection, isolated a stable pool of cells by flow sorting, and compared insulin-stimulated externalization in these cells and in 3T3-L1 preadipocytes. As shown in Fig. 4a, the NIH 3T3 cells respond poorly to insulin stimulation, with a less than twofold increase in the proportion of GLUT4 at the cell surface. In contrast, the 3T3-L1 preadipocytes demonstrate a rapid externalization, such that the increase in cell surface GLUT4 reached almost fourfold at 5 min after insulin addition. Subsequently, the proportion of GLUT4 at the cell surface decreases markedly, so that the first phase of the response overshoots the final steady state. The data are consistent with the presence of a highly insulin-responsive pool of GLUT4 in the basal state in 3T3-L1 preadipocytes but not in NIH 3T3 cells. After the initial, rapid mobilization (and depletion) of this pool, the 3T3-L1 preadipocytes may be only marginally able to recycle GLUT4 faster than NIH 3T3 cells, so that the difference in steady-state presence of insulin is minimal. We also expressed the GLUT4 reporter in a cultured, nontransformed hepatocyte cell line (AML12 [110]) and found that in these cells as well,

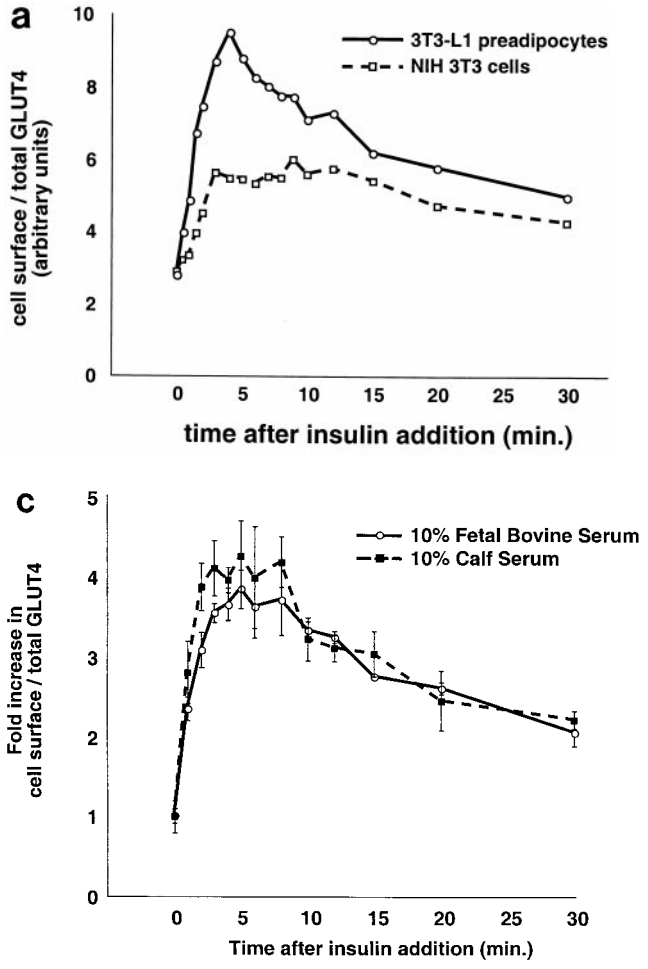

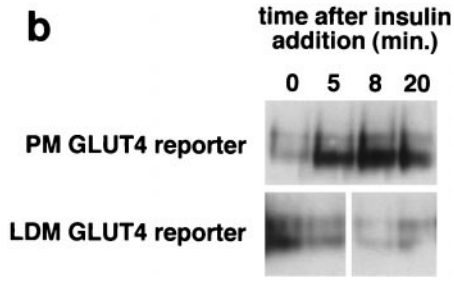

FIG. 4. Kinetics of GLUT4 trafficking in 3T3-L1 preadipocytes and NIH 3T3 cells. (a) Confluent 3T3-L1 preadipocytes and NIH 3T3 cells expressing similar amounts of the reporter were treated with 160 nM insulin for various lengths of time, chilled, and analyzed by FACS to measure changes in the proportion of GLUT4 reporter present at the cell surface. Insulin caused a much more marked redistribution of GLUT4 to the plasma membrane of 3T3-L1 preadipocytes than of NIH 3T3 cells. (b) Translocation of the GLUT4 reporter in 3T3-L1 preadipocytes was assayed by subcellular fractionation and immunoblotting. After serum starvation, cells were stimulated with 480 nM insulin (added from a prewarmed 3× stock) for various amounts of time, then washed with cold PBS^{++}, and fractionated as described in Materials and Methods. Equal amounts of protein were loaded in each lane. Insulin caused an increase in the amount of GLUT4 reporter in the plasma membrane (PM) fraction, with a peak response at 8 min after insulin addition and a subsequent decrease at 20 min. A reciprocal pattern is apparent in the low-density microsomal (LDM) fraction. The experiment was performed twice, with similar results each time. (c) Confluent 3T3-L1 preadipocytes were cultured for 3 days in either 10% fetal bovine serum or 10% calf serum. Cells were then starved, stimulated with 160 nM insulin for various amounts of time, and analyzed by flow cytometry. Samples were measured in duplicate (control samples were in triplicate or quadruplicate). Insulin caused similar increases in the fraction of GLUT4 reporter at the plasma membrane under both conditions. The experiment was done twice, with similar results each time.

insulin stimulated minimal translocation and there was no overshoot (not shown). We conclude that insulin regulates GLUT4 recycling through a highly insulin-responsive mechanism present in 3T3-L1 adipocytes and, at least to some degree, in 3T3-L1 preadipocytes, but not characteristic of all cell types.

To further demonstrate that insulin mobilizes GLUT4 to the plasma membrane of 3T3-L1 preadipocytes, we performed subcellular fractionation and immunoblotting. Since native GLUT4 is not expressed in undifferentiated 3T3-L1 cells, we used cells expressing the GLUT4 reporter. As shown in Fig. 4b, insulin stimulates movement of the GLUT4 reporter out of the LDM fraction and into the PM fraction. The peak response is at 8 min after insulin addition. By 20 min there is a decrease from this peak in the PM fraction as well as a slight increase in the amount present in the LDM fraction. These subcellular fractionation data not only indicate that the GLUT4 reporter is translocated in 3T3-L1 preadipocytes, but also suggest that there is an early overshoot before the final steady-state response. Thus, the subcellular fractionation data are in accord with our flow cytometry data.

One possible explanation for why we observe GLUT4 translocation in 3T3-L1 preadipocytes where others have not is that we routinely culture these cells in 10% fetal bovine serum rather than the more usual 10% calf serum. We therefore cultured confluent 3T3-L1 preadipocytes in each of these sera for 3 days prior to assaying the effect of insulin on GLUT4 trafficking. As shown in Fig. 4c, cells cultured in 10% calf serum and in 10% fetal bovine serum responded indistinguishably. In both cases, insulin causes a fourfold increase in the fraction of GLUT4 present at the plasma membrane at early (5 min) time points, with a subsequent decrease, as previously noted. These data are consistent with the those presented in Fig. 3a and 4a and indicate that the effect that we observed does not result from culture of 3T3-L1 preadipocytes in fetal bovine serum.

Kinetics of insulin-stimulated GLUT4 translocation in CHO cells are medium dependent. To determine if the kinetics of insulin-stimulated GLUT4 externalization are similar in CHO cells and in 3T3-L1 cells, we assayed changes in the proportion of GLUT4 at the cell surface of CHO cells stimulated for various amounts of time. To parallel the conditions used for 3T3-L1 cells, some CHO cells were placed in DMEM 2 days before the experiment; others were left in standard CHO medium (F12). As shown in Fig. 5, CHO cells cultured in DMEM respond to insulin with a dramatic, biphasic redistribution of GLUT4 to the cell surface. In contrast, CHO cells cultured in F12 medium redistributed GLUT4 less dramatically and with no overshoot of the final steady-state proportion

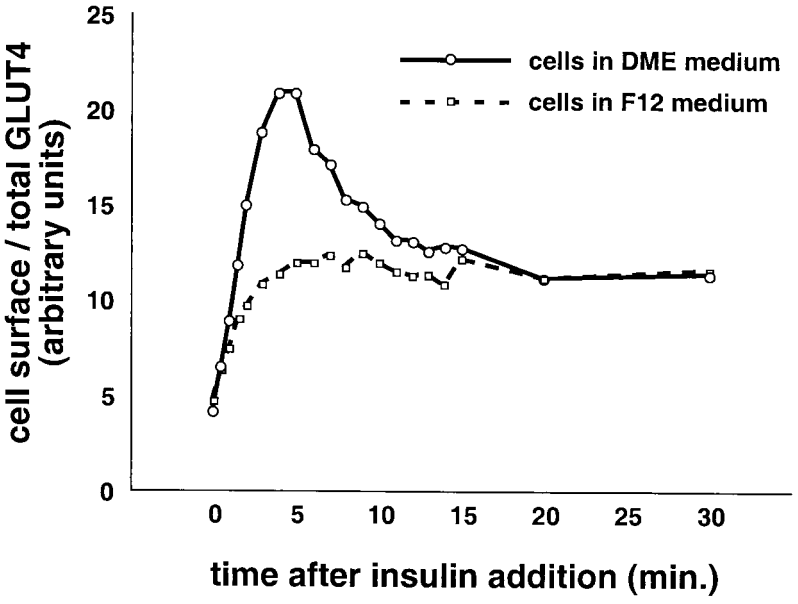

FIG. 5. Culture conditions modulate the kinetics of insulin-stimulated GLUT4 translocation in CHO cells. Two days before the experiment, confluent CHO cells were placed in DMEM identical to that used for 3T3-L1 adipocytes or left in F12 culture medium. Cells were starved overnight before the experiment. On the day of the experiment, cells were stimulated with 80 nM insulin for 0, 0.5, 1, 1.5, 2, 3, 4, 5, 6, 7, 8, 9, 10, 11, 12, 13, 14, 15, 20, or 30 min, then transferred to 4°C, and washed with cold PBS. Staining and flow cytometry were done as described in the text. For cells cultured in DMEM, insulin stimulated a rapid increase in GLUT4 reporter present at the cell surface, peaking at 4 to 5 min after insulin addition. Subsequently, the proportion of GLUT4 on the plasma membrane decreases, and a steady state in the presence of insulin is reached 20 min after insulin addition. In contrast, cells cultured in F12 medium externalized GLUT4 with monophasic kinetics, characterized by no overshoot of the final steady-state response in the presence of insulin. Both the initial and final proportions of GLUT4 at the cell surface are essentially unaffected by the culture conditions, despite the marked effect on intermediate time points. For cells cultured in DMEM, the peak response is a 5.5-fold increase in the proportion of GLUT4 at the cell surface compared to the basal state. The kinetics and the amplitude of the peak response are similar in CHO cells cultured in DMEM and in 3T3-L1 cells (compare to Fig. 3a, 4a, and 4c).

of GLUT4 at the cell surface in the presence of insulin. As with 3T3-L1 cells, GLUT4 externalization in DMEM-cultured CHO cells peaks at 4 to 5 min after insulin addition and then decreases to reach a steady state by 20 min after insulin addition. The peak fraction of GLUT4 at the cell surface is 5.5-fold more than that in unstimulated cells, and in several experiments 50 to 60% of this increase is eliminated in the subsequent decrease. For comparison, the peak response of 3T3-L1 adipocytes in Fig. 3a was 5.4-fold over basal (average of days 8 and 10), though the subsequent decrease to steady state was only ~20% of this peak response.

To examine the subcellular distribution of the GLUT4 reporter in CHO cells cultured in these two distinct media, we performed immunofluorescence microscopy. Cells were cultured in F12 or DMEM for 2 days, stimulated with insulin for 0, 5, or 20 min, chilled, and stained without permeablization to detect the externalized Myc epitope tag. As shown in Fig. 6a, cells cultured in F12 have a small increase in the amount of externalized Myc epitope at 5 and significantly more at 20 min after insulin addition (top row). In contrast, cells cultured in DMEM have greater cell surface staining at 5 min than at 20 min after insulin addition (third row); after 5 min of insulin treatment, the amount of surface Myc-GLUT4 fluorescence is much greater in cells cultured in DMEM than in F12. We also examined the distribution of GLUT4 reporter within the cells using GFP fluorescence. In this case, we noted that cells cultured in F12 have an abundance of the reporter protein in the perinuclear region, both in the absence of insulin and after 5 or 20 min of insulin treatment (second row). In cells cultured in DMEM, this perinuclear accumulation is less marked (fourth row). Though these microscopy data are more difficult to quantify accurately than the flow cytometry data (Fig. 5), it is clear that the kinetics that we observe by microscopy are similar to those observe using flow cytometry.

Figure 6b presents a higher magnification demonstrating the intracellular distribution of the GLUT4 reporter in CHO cells cultured in these two distinct media. In the basal state, GLUT4 is prominent in the perinuclear region in cells cultured in F12 medium (Fig. 6b, lower left panel, arrowheads). In contrast, cells cultured for 2 days in DMEM have less GLUT4 in the perinuclear region and more that is present in punctate structures in the periphery (upper left panel). Insulin treatment for 5 min causes a dramatic increase in plasma membrane GLUT4 in cells cultured in DMEM (Fig. 6b, arrows, upper center panel). Cells cultured in F12 have a less marked accumulation of GLUT4 at the plasma membrane after 5 min of insulin treatment (Fig. 6b, lower center panel). By 20 min after insulin addition, the amount of GLUT4 at the plasma membrane is similar in cells cultured in both media and is less than the peak response at 5 min of insulin treatment for cells cultured in DMEM (right panels of Fig. 6b). Of note, cells cultured in F12 medium have continued prominent perinuclear GLUT4 accumulation even after 5 or 20 min of insulin treatment (Fig. 6b,

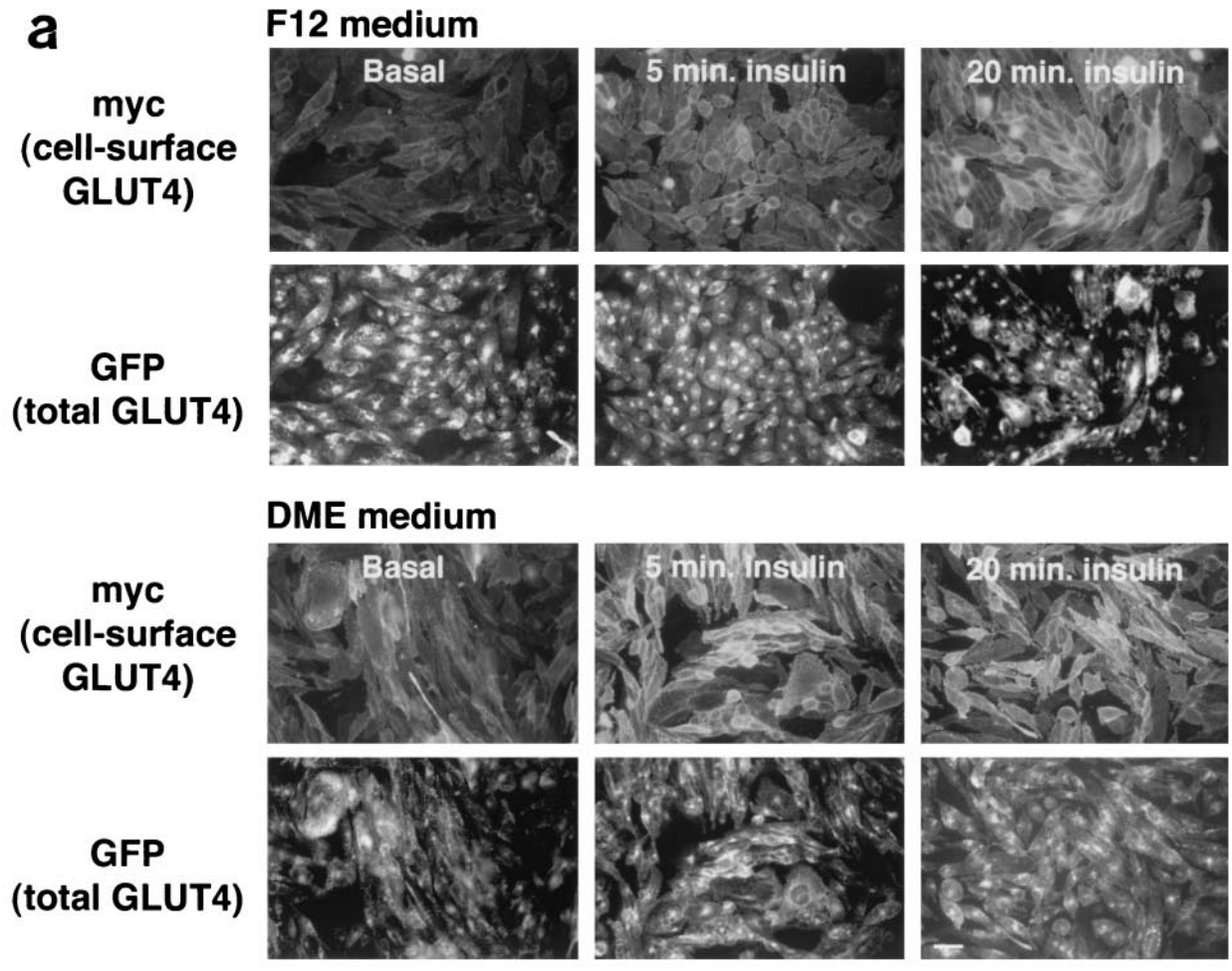
a
F12 medium
Basal
5 min. insulin
20 min. insulin
myc
(cell-surface
GLUT4)
GFP
(total GLUT4)
DME medium
Basal
5 min. insulin
20 min. insulin
myc
(cell-surface
GLUT4)
GFP
(total GLUT4)

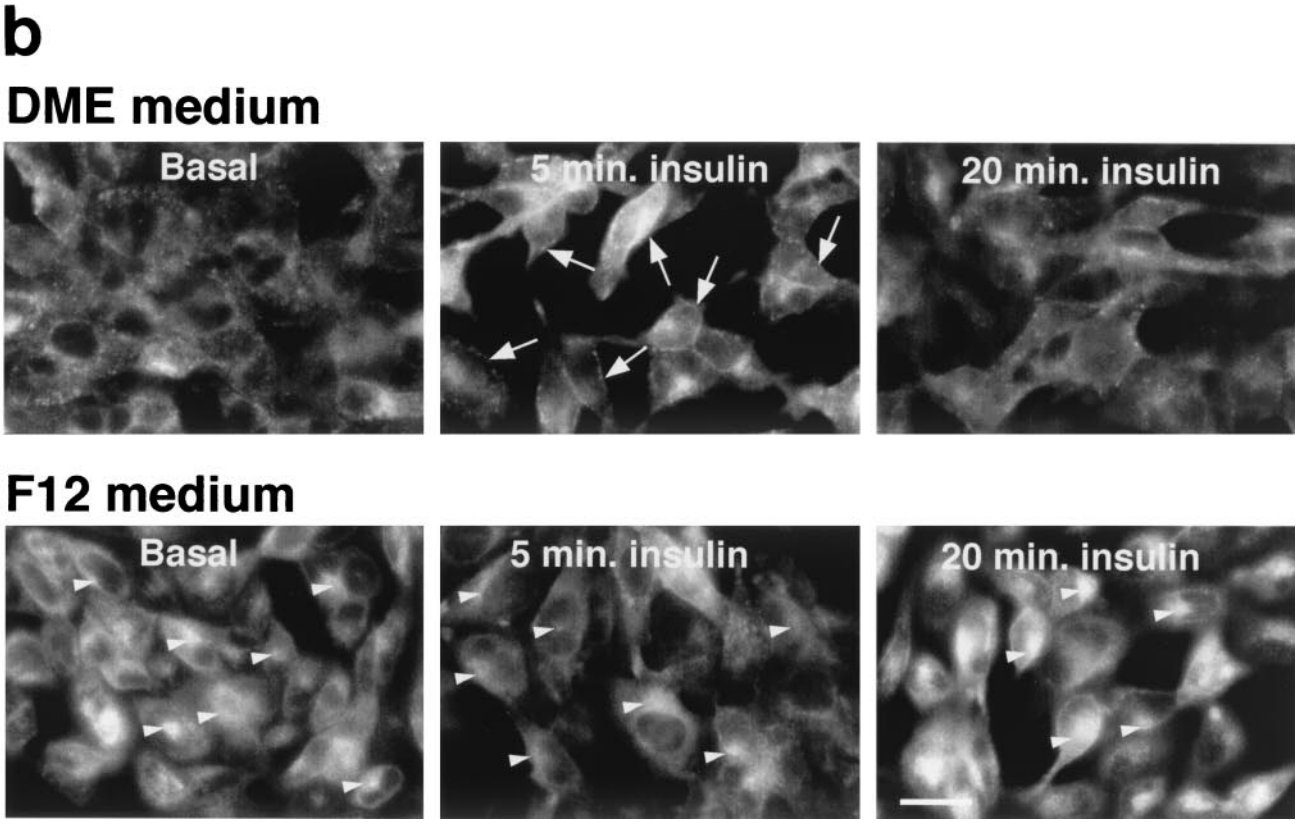
b
DME medium
Basal
5 min. insulin
20 min. insulin
F12 medium
Basal
5 min. insulin
20 min. insulin

arrowheads, lower center and right panels). These data are consistent with the flow cytometry data presented in Fig. 5. Thus, correlation of kinetic and microscopy data suggests that GLUT4 accumulates in a peripheral, highly insulin-responsive compartment in the basal state when the cells are cultured in DMEM. The perinuclear GLUT4 accumulation seen in the cells cultured in F12 may represent a longer-term reservoir. Finally, the overshoot of the steady-state proportion of GLUT4 at the cell surface in the presence of insulin corresponds, to a first approximation, to the amount of GLUT4 that has accumulated in the peripheral compartment in CHO cells.

Amino acid sufficiency modulates highly insulin-responsive GLUT4 trafficking in CHO cells and in 3T3-L1 adipocytes. DMEM and F12 medium differ in several respects. Though DMEM has greater glucose and calcium concentrations, neither of these components alone or in combination proved necessary or sufficient to cause highly insulin-responsive (i.e., biphasic) kinetics (data not shown). We noted that many essential amino acids are present at markedly higher concentrations in DMEM than in F12 (see above) and tested the possibility that these are required for highly insulin-responsive GLUT4 trafficking. After culture for 24 to 36 h in various media, we examined the kinetics of insulin-stimulated GLUT4 translocation in CHO cells. As shown in Fig. 7a, the degree of overshoot of the final steady-state response in the presence of insulin correlates quite well with the concentration of most essential amino acids in different media. DMEM has twofold the concentrations of most amino acids present in MEM, which in turn has 2- to 12-fold greater concentrations of most amino acids than F12. In MEM made without any amino acids, we observed no overshoot of the final, steady-state proportion of GLUT4 at the plasma membrane in the presence of insulin. We also tested the kinetics of GLUT4 externalization in CHO cells cultured in MEM with 2×, 1×, 0.2×, or no amino acids, as shown in Fig. 7b. Higher concentrations of amino acids result in a greater overshoot of the final steady-state response in the presence of insulin. Since glutamine was held constant, we surmise that flux through the glucosamine pathway is not likely to be responsible for this effect.

Another insulin signaling output that is sensitive to amino acid availability is the phosphorylation of p70 S6-kinase (28). In this case, withdrawal of most individual amino acids inhibits the ability of insulin to stimulate p70 phosphorylation to various degrees; the most potent were leucine and arginine, and the effect was mimicked by rapamycin. We also observed a modest decrease in the proportion of GLUT4 rapidly mobilized by insulin in CHO cells cultured without leucine and arginine (not shown). More striking is the ability of rapamycin to alter the kinetics of insulin-stimulated GLUT4 externalization. As shown in Fig. 8, rapamycin used over a range of concentrations progressively eliminated the rapid first phase of insulin-stimulated GLUT4 externalization, so that at the highest concentration there was no overshoot of the final steady-state response. Of note, the amount of GLUT4 reporter protein, as assessed by GFP fluorescence, did not change by more than ~10% after amino acid deprivation or rapamycin treatment (not shown). These data parallel those presented in Fig. 7 and indicate that amino acid sufficiency modulates GLUT4 targeting to a highly insulin-responsive compartment through a rapamycin-sensitive mechanism.

To learn whether our observations in CHO cells are relevant to GLUT4 trafficking in 3T3-L1 adipocytes, we varied the amino acid concentrations in which fully differentiated 3T3-L1 adipocytes expressing the reporter were cultured. After 36 h, we examined the externalization of GLUT4 after insulin addition. As shown in Fig. 9, 3T3-L1 adipocytes cultured in MEM with 2× amino acids (relative to standard MEM and similar to DMEM) mobilized GLUT4 similarly to cells cultured in DMEM (e.g., Fig. 3a). Strikingly, culture in progressively lower concentrations of amino acids resulted in decreased magnitude of GLUT4 translocation (Fig. 9). In all cases, the overshoot of the steady-state response remains intact, even in the absence of amino acids (except glutamine). Indeed, for 3T3-L1 adipocytes cultured in the absence of amino acids, the response demonstrates a marked overshoot followed by only a modest fold increase in GLUT4 at the cell surface in the steady state; this is somewhat reminiscent of the response we observed using CHO cells cultured in DMEM (Fig. 5). Culture of 3T3-L1 cells in the presence of

FIG. 6. Culture conditions modulate the subcellular distribution of GLUT4 in CHO cells. CHO cells expressing the GLUT4 reporter were plated on coverslips, allowed to reach confluence, and then treated as described in the legend to Fig. 5. Two days before microscopy, cells were changed to DMEM or continued in F12 culture medium. On the day of microscopy, cells were serum starved for 3 h and then stimulated with 160 nM insulin for the times indicated. (a) Cells were chilled and stained without fixation or permeablization to detect externalized Myc epitope tag. A red (Alexa594-conjugated) secondary antibody was used, and the images are shown in the first (F12) and third (DMEM) rows. GFP was used to detect the total cellular GLUT4 reporter, and images are shown in green in the second (F12) and fourth (DMEM) rows. Cells cultured in F12 medium have the greatest amount of GLUT4 at the cell surface at 20 min, whereas those cultured in DMEM have more at the cell surface at 5 min. Scale bar, 10 μm. (b) The subcellular distribution of the GLUT4 reporter is more closely examined. These cells were fixed, permeablized, and stained with anti-Myc antibody and a FITC-conjugated secondary antibody in order to increase the total green fluorescent signal, which is then due to the combination of GFP and FITC. In cells cultured in F12, there is prominent staining of the GLUT4 reporter in the perinuclear region; this does not change significantly with short-term insulin treatment (bottom panels, arrowheads). In contrast, the GLUT4 reporter is absent from the perinuclear region in unstimulated cells cultured in DMEM and is present more prominently in punctate, peripheral structures (top left panel). Insulin treatment for 5 min results in a dramatic accumulation of GLUT4 at the plasma membrane in the cells cultured in DMEM (top center panel, arrows). In contrast, cells cultured in F12 medium have much less plasma membrane GLUT4 after 5 min of insulin treatment (bottom center panel). By 20 min after insulin addition, plasma membrane GLUT4 is similar in cells cultured in the two culture media (top right and bottom right panels) and is less prominent than at 5 min in the cells cultured in DMEM (compare to top center panel). The changes observed at the plasma membrane by microscopy correlate well with those quantified by flow cytometry (Fig. 5). Additionally, microscopy demonstrates that when the cells are cultured in DMEM rather than F12 medium, GLUT4 is distributed away from the perinuclear region and into punctate structures in the periphery. Scale bar, 10 μm.

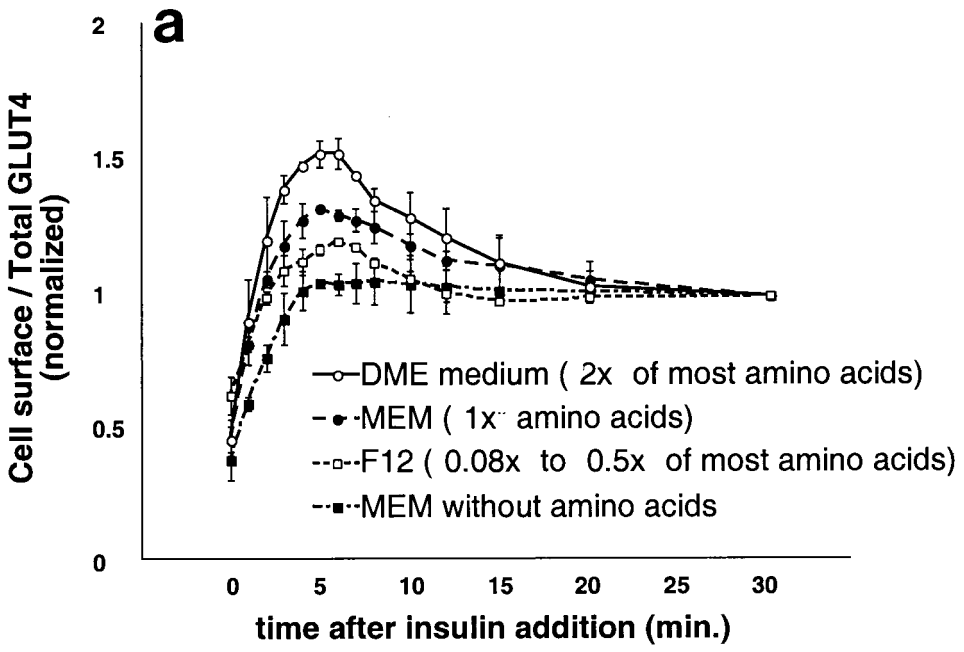

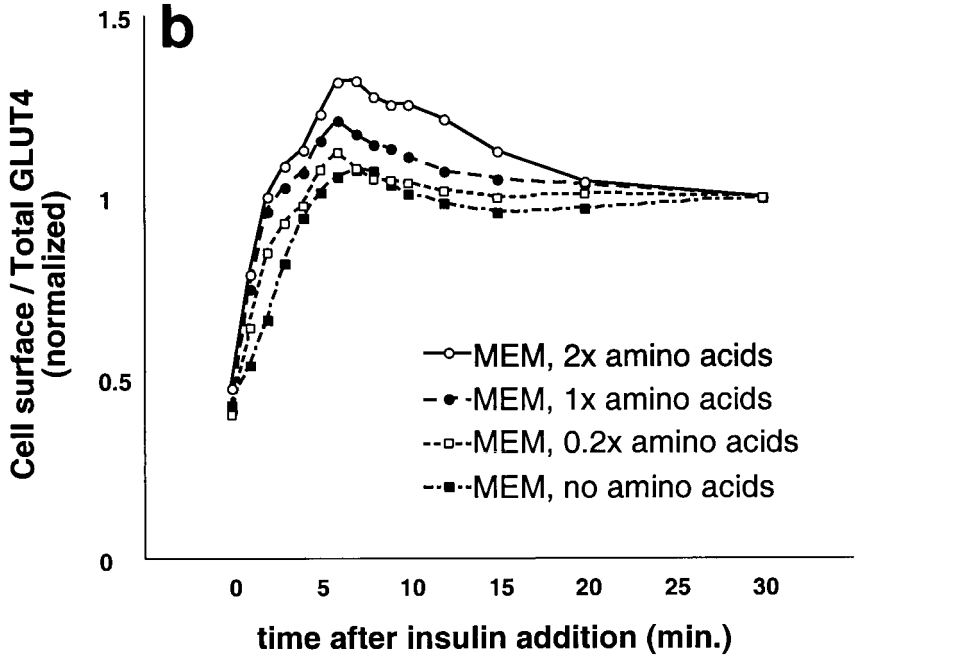

FIG. 7. Amino acid concentrations regulate the amount of rapidly insulin-mobilized GLUT4 in CHO cells. (a) CHO cells expressing the reporter were cultured in the indicated media for 36 h and serum starved during the last 12 h of this period. Cells were stimulated with 160 nM insulin for various amounts of time, then chilled, stained for externalized Myc epitope tag, and analyzed by FACS as described in the text to determine the relative proportion of GLUT4 at the cell surface in each sample. Compared to the amino acid concentrations in standard MEM (defined as 1× amino acids), concentrations of most amino acids in DMEM are twofold higher, and concentrations of most amino acids in F12 are only 0.08 to 0.5 times as high (depending on the particular amino acid; see Materials and Methods). All media contained 2 mM glutamine. The degree to which insulin stimulates a transient overshoot of the final, steady-state proportion of GLUT4 at the plasma membrane correlates well with the concentrations of essential amino acids in the various media. The data shown are from two separate experiments (mean ± standard deviation) and are normalized to the steady-state response in the presence of insulin (30-min time point). (b) A similar experiment was performed with cells cultured in MEM containing various concentrations of essential amino acids except for glutamine, which was held constant (see text). Higher amino acid concentrations cause a greater overshoot of the final, steady-state fraction of GLUT4 at the plasma membrane after insulin addition.

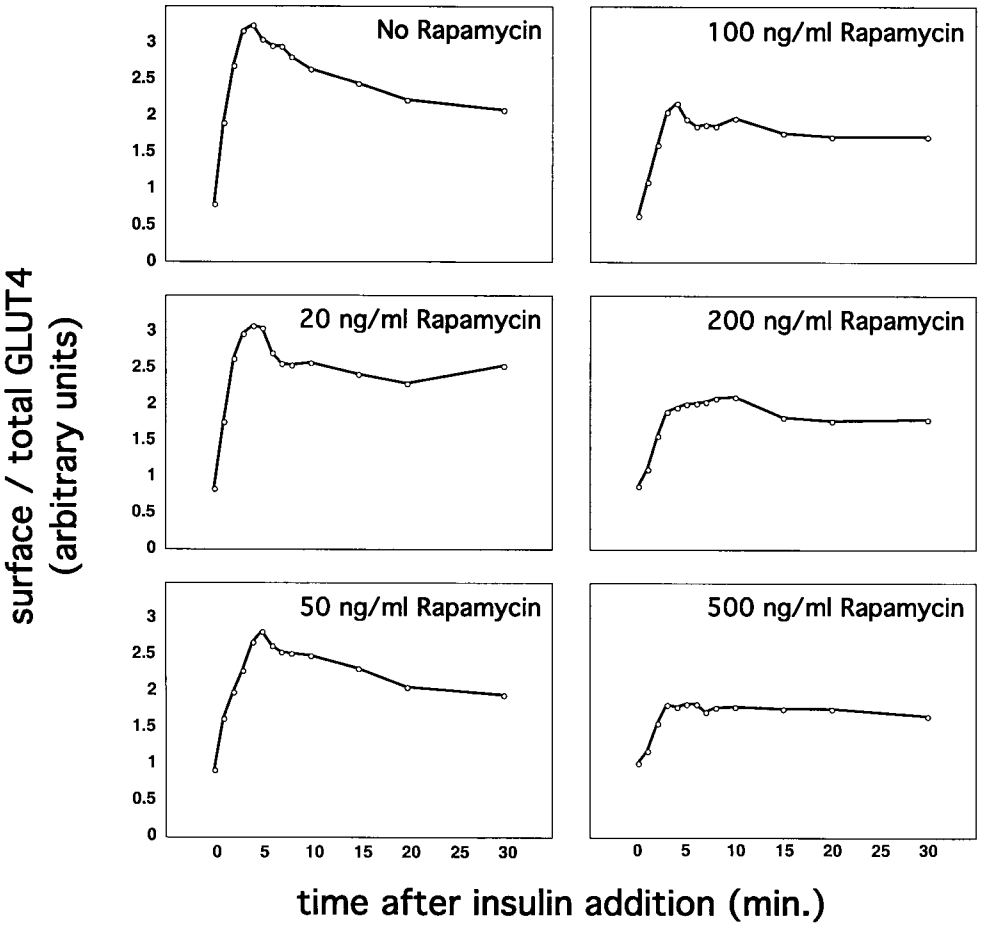

FIG. 8. Rapamycin treatment diminishes the amount of rapidly insulin-mobilized GLUT4 in CHO cells. CHO cells expressing the GLUT4 reporter were cultured in DMEM, treated with the indicated concentrations of rapamycin for 36 h, and serum starved during the last 12 h of this period. Cells were stimulated with 160 nM insulin for the indicated times, then chilled, stained for externalized Myc epitope, and subjected to flow cytometry to determine the relative proportion of GLUT4 at the cell surface in each sample. Increasing concentrations of rapamycin caused a progressive diminution of the first phase of GLUT4 externalization (i.e., the overshoot before the steady-state response). Simultaneously, the proportion of GLUT4 at the cell surface in the basal state increased slightly but progressively with increasing rapamycin concentration. Together with the data presented in Fig. 7, these data show that amino acid abundance regulates the amount of rapidly insulin-translocated GLUT4 in CHO cells through a rapamycin-sensitive mechanism.

rapamycin has a similar effect, as shown in Fig. 10. Here, a progressive increase in the concentration of rapamycin caused a progressive decrease in the magnitude of GLUT4 translocation by insulin. As with amino acid insufficiency, rapamycin treatment of 3T3-L1 adipocytes does not alter the presence of biphasic kinetics. Finally, the amount of GLUT4 reporter present in each cell, as assessed by GFP fluorescence, did not decrease by more than 10% after amino acid starvation or rapamycin treatment (not shown). Overall, the data are consistent with the notion that amino acid sufficiency modulates GLUT4 trafficking through a kinetically defined, highly insulin-responsive compartment in 3T3-L1 adipocytes and that this effect is rapamycin sensitive.

DISCUSSION

We have shown that insulin triggers rapid exocytosis of GLUT4 in 3T3-L1 adipocytes and preadipocytes and in CHO cells, but not in NIH 3T3 cells. This conclusion is based on studies using a novel, FACS-based assay to measure changes in the proportion of GLUT4 present at the plasma membrane and is supported by subcellular fractionation data. This action of insulin is blocked by either of two structurally dissimilar phosphatidylinositol-3-kinase inhibitors in 3T3-L1 cells at all times during differentiation, suggesting that identical signaling mechanisms are involved. Moreover, insulin stimulates GLUT4 externalization with identical, biphasic kinetics at all times during 3T3-L1 differentiation, and we demonstrate reinternalization and recycling of the reporter protein as well. Strikingly, we find that when CHO cells are cultured identically to 3T3-L1 adipocytes (in DMEM), the kinetics and initial magnitude of insulin-stimulated GLUT4 redistribution are similar in both cell types. In contrast, when CHO cells are cultured in their usual medium (F12), GLUT4 is only minimally distributed to a highly insulin-responsive compartment, assessed kinetically. The presence of GLUT4 in this rapidly mobilized compartment correlates with a basal-state redistribution of

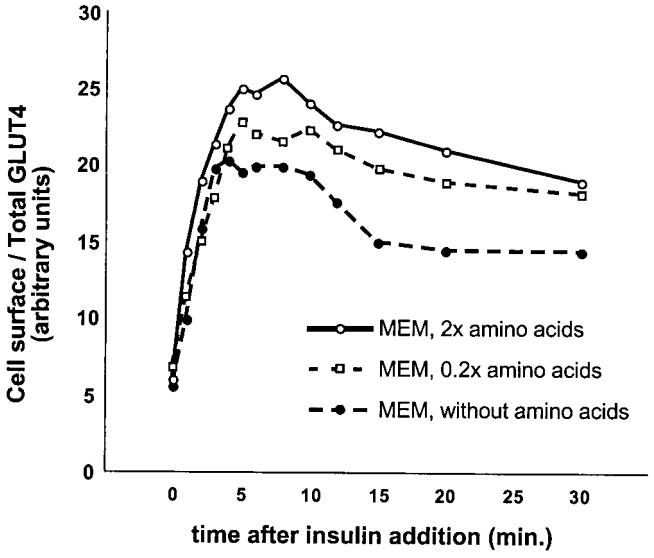

FIG. 9. Amino acid sufficiency modulates insulin-stimulated GLUT4 translocation in 3T3-L1 adipocytes. 3T3-L1 adipocytes expressing the GLUT4 reporter were cultured in MEM with the indicated concentrations of amino acids for 36 h and serum starved during the last 12 h. Cells were stimulated with 160 nM insulin for the indicated times, then chilled, stained for externalized Myc epitope tag, and analyzed by flow cytometry to determine the relative proportion of GLUT4 at the cell surface in each sample. MEM with 2× amino acids approximates the amino acid concentrations found in DMEM (see Materials and Methods). Culture of the cells in media with poor amino acid availability results in reduced translocation of GLUT4 to the cell surface after insulin stimulation.

GLUT4 out of the perinuclear region and into punctate structures in the periphery. We next demonstrate that the difference in GLUT4 targeting in these two media is, at least in part, due to a difference in amino acid concentrations. Thus, our data indicate that in CHO cells cultured with abundant amino acids, GLUT4 accumulates in a peripheral compartment that is rapidly mobilized after insulin addition. Conversely, in low amino acid concentrations, GLUT4 may be targeted primarily to the endosomal system or the trans-Golgi reticulum. We show that rapamycin can inhibit the ability of amino acids to cause GLUT4 accumulation in a highly insulin-responsive compartment in CHO cells. Finally, we find that amino acid concentrations also modulate GLUT4 trafficking in 3T3-L1 adipocytes and that this effect is also rapamycin sensitive.

Assay for GLUT4 trafficking at the cell surface. Several assays for GLUT4 trafficking at the cell surface have been described. The subcellular fractionation protocol pioneered by Cushman and colleagues provided the first evidence that glucose uptake is regulated by redistribution of glucose transporters to the plasma membrane (15, 102). However, the use of subcellular fractionation to measure cell surface GLUT4 is laborious, and accurate quantitation has been difficult because of cross-contamination of plasma membrane fractions (35). The use of photoactivatable bismannose compounds to selectively tag cell surface glucose transporters allowed improved quantitation as well as measurement of steady-state internalization and externalization rate constants in the basal and insulin-stimulated states (10, 14, 35, 36, 85, 113). Yet this approach, too, is laborious and requires quantitative immunoprecipitation and analysis by SDS-PAGE. The preparation of plasma membrane sheets, followed by immunostaining for GLUT4 and fluorescence microscopy, is at best semiquantitative (50, 59, 63, 79).

Expression of an exogenous, tagged GLUT4 reporter offers greater flexibility in detection and quantitation. Ebina and others have shown that an epitope tag in the first exofacial loop allows detection of a GLUT4 reporter on the surface of intact cells and that changes in the amount present can be easily quantified (44, 75, 108). Other investigators fused GLUT4 to GFP and observed insulin-regulated trafficking in individual cells by fluorescence microscopy (18, 67, 104). We and others have described the use of these tags in combination (54; J. S. Bogan and H. F. Lodish, Abstr. 38th Annu. Meet. Am. Soc. Cell Biol., abstr. L65, 1998). The level of expression of such reporter proteins is critical; significant overexpression of a GLUT4 reporter in primary rat adipose cells results in saturation of the trafficking mechanism, with decreased insulin responsiveness (2). Indeed, significant overexpression in 3T3-L1 adipocytes might be one reason that insulin stimulated a relatively low increase in cell surface epitope-tagged GLUT4 in the original study (44).

We present here the first detailed characterization of a GLUT4 reporter with both an exofacial epitope tag and GFP fused to the cytosolic tail. The assay that we describe represents a significant advance over previous metrics because it allows accurate quantification of changes in the proportion—

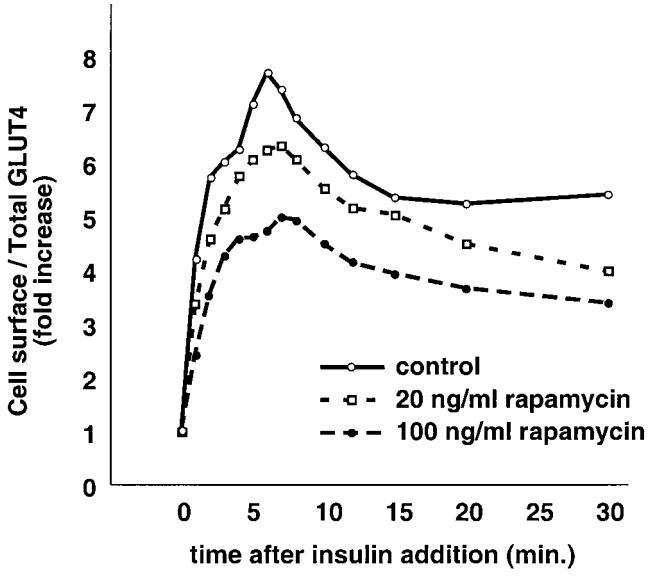

FIG. 10. Rapamycin treatment diminishes insulin-stimulated GLUT4 translocation in 3T3-L1 adipocytes. 3T3-L1 adipocytes expressing the GLUT4 reporter were cultured in DMEM with the indicated concentrations of rapamycin for 36 h and starved for the final 12 h of this period. Cells were then stimulated with 160 nM insulin for the indicated amounts of time, chilled, stained to detect externalized Myc epitope, and subjected to FACS to determine the relative proportion of GLUT4 at the cell surface in each sample. In the presence of increasing concentrations of rapamycin, GLUT4 was translocated to progressively fewer degrees by insulin stimulation.

rather than the amount—of GLUT4 that is present at the cell surface. These measurements are made on a cell-by-cell basis using flow cytometry, with the result that alterations in cell surface GLUT4 targeting are determined with high specificity and precision. Importantly, we show that this reporter protein codistributes with native GLUT4, that native GLUT4 coimmunopurifies with vesicles containing the reporter, and that the reporter is reinternalized after insulin removal and recycles to the plasma membrane upon restimulation. The time course for GLUT4 reinternalization is slightly prolonged in 3T3-L1 adipocytes compared to fibroblasts; this may be because adipocytes express a greater number of insulin receptors, which are endocytosed with bound insulin (78). Thus, insulin removal may not effectively stop insulin signaling in adipocytes. We have been careful to isolate a stable population of cells that express a moderate amount of the reporter protein so as to avoid saturation of the trafficking mechanism. The use of flow cytometry, as well as the presence of several tandem epitope tags, nonetheless enables us to measure small amounts of cell surface and total reporter. Finally, our method allows rapid analysis of multiple samples, making possible the detailed kinetic studies that we present here.

Kinetics of GLUT4 mobilization after insulin addition. Using this novel, FACS-based assay to measure the relative proportion of GLUT4 at the cell surface, we present detailed kinetic data characterizing the insulin responsiveness of various cell types. In 3T3-L1 preadipocytes and adipocytes as well as in CHO cells, insulin causes a rapid ~5-fold increase in plasma membrane GLUT4, peaking at about 5 min. Cell surface GLUT4 then declines until a steady-state level is reached at about 15 min. We also detected this transient overshoot in cell surface GLUT4 using uninfected 3T3-L1 adipocytes and subcellular fractionation to study the endogenous protein. In the fractionation data, the peak occurs slightly later (7 min), possibly because of the difficulty in synchronizing the responses of a large number of cells (several 10-cm dishes) required for biochemical analysis. By comparison, the FACS-based assay is done in a six-well-plate format. It seems more likely that all of the cells in a single well will behave as a synchronized cohort; if so, the FACS data may be the more accurate kinetic measurement.

A second possible explanation for the slightly faster kinetics that we observed using the FACS-based assay compared to subcellular fractionation could be transient trafficking of GLUT4 through caveolae. GLUT4 present in these Triton-insoluble plasma membrane domains might not be detected using our fractionation and immunoblotting protocol, yet an externalized Myc epitope tag would presumably still be detected by cell surface staining of intact cells. Whether or not GLUT4 traffics through caveolae remains uncertain, and data have been reported both in favor of and against this possibility (26, 47, 86). Recent work indicates that mobilization of GLUT4 requires signaling through a CAP-Cbl complex that localizes transiently in Triton-insoluble, caveolin-enriched plasma membrane subdomains after insulin stimulation (6). These data are broadly consistent with the notion that GLUT4 may also traffic transiently through such domains during insulin-stimulated exocytosis. Such a phenomenon might also help to explain observations that GLUT4 may under some circumstances be present in the plasma membrane without a corresponding increase in glucose uptake (33, 49, 106, 111).

Our data could be consistent with a biphasic effect on either GLUT4 exocytosis or endocytosis. We favor the former interpretation because of biochemical and immunoelectron microscopy data indicating that, in adipocytes, GLUT4 is sequestered from endosomes into a highly insulin-responsive, TfnR-negative and CD-M6PR-negative pool (1, 32, 46, 55, 57, 64, 65, 76). Insulin acts primarily to mobilize this sequestered pool of GLUT4 to the cell surface. Thus, in the absence of insulin, the exocytosis rate is limited by sequestration and accumulation of GLUT4 in the insulin-responsive compartment. After insulin addition, the GLUT4 that has accumulated in this compartment is mobilized, and the compartment itself is depleted of GLUT4. Importantly, the rate of GLUT4 exocytosis in the steady-state presence of insulin is now limited at some other step in the recycling pathway; this could be trafficking from endosomes to the insulin-responsive compartment or directly to the cell surface (37, 114). Recent analyses also suggest the presence of a unique GLUT4 storage compartment and suggest that traffic through this compartment to the highly insulin-responsive exocytic compartment may be rate limiting for exocytosis in the steady-state presence of insulin (55, 56). This notion may fit with other recent work demonstrating that GFP-tagged GLUT4 proteins move to the cell surface directly from the perinuclear region, which may be a storage compartment, in 3T3-L1 adipocytes (70). In either case, the relative amount of GLUT4 present in the highly insulin-responsive compartment of unstimulated cells can be assessed indirectly, as the amount of GLUT4 translocated immediately (in the first 5 min) after insulin addition (i.e., before steady state is reached).

The above reasoning forms the rationale for our focus on the biphasic kinetics of GLUT4 translocation in insulin-responsive cells. The first phase of the response (the overshoot before the steady state) represents mobilization of GLUT4 that has accumulated in the insulin-responsive pool. The second phase (the steady state in the presence of insulin, after 15 to 20 min) is determined by trafficking rates that do not inform us of the initial size of the insulin-responsive pool. The initial overshoot of the steady-state GLUT4 distribution after insulin stimulation was predicted by mathematical analysis, but measurement of GLUT4 or IRAP in plasma membranes by subcellular fractionation or photolabeling did not convincingly demonstrate its occurrence (14, 37, 74, 81, 85, 111). Likewise, older studies of glucose uptake and cytochalasin B binding failed to detect a biphasic response (49, 52, 53). Our observation of this phenomenon may reflect an improved sensitivity of our FACS assay. However, we were also able to detect this initial overshoot in cell surface GLUT4 using uninfected 3T3-L1 adipocytes and subcellular fractionation. We do not know why this response has not been detected previously, though clearly the details of insulin stimulation are important. In experiments examining native GLUT4, we used high concentrations of insulin added from a prewarmed 3× stock to simultaneously and maximally stimulate all of the cells in the population. We would probably have not stimulated cells this way were it not for our FACS results, which we sought to confirm. Another consideration is that the divergent results may be due to dif-

ferences between 3T3-L1 cells and primary rat adipocytes, which were used for many previous kinetic studies. Our measurement of the initial rate of GLUT4 externalization is more rapid than that reported by Clark et al. (14) and Patki et al. (70) but is quite similar to data of Satoh et al. (14, 70, 85). Indeed, careful examination of the latter group's data suggests a slight overshoot of the insulin-stimulated steady-state response in primary rat adipocytes, though at the time this appears to have been attributed to uncertainty in the measurement (see Fig. 6A of Satoh et al. [85]).

Cell type specificity of GLUT4 trafficking. Using the assay described here, we initially observed highly insulin-responsive GLUT4 trafficking in differentiated and undifferentiated 3T3-L1 cells and in CHO cells, leading us to suggest that machinery required for insulin-responsive GLUT4 trafficking might not be exclusive to adipose and muscle (J. S. Bogan and H. F. Lodish, Abstr. 38th Annu. Meet. Am. Soc. Cell Biol., abstr. L65, 1998). Very recently, similar results led others to conclude that undifferentiated fibroblasts possess the requisite mechanism (54). Our data demonstrate that this is not the case. We find that a highly insulin-responsive pool containing GLUT4 is present in fully differentiated 3T3-L1 adipocytes but absent in NIH 3T3 cells. This conclusion is based as much on the presence of the overshoot as it is on the magnitude of the increase in cell surface GLUT4 after insulin addition to 3T3-L1 adipocytes. After insulin treatment of NIH 3T3 cells, we observed neither the overshoot nor a large increase in cell surface GLUT4, consistent with the generally held notion that a highly insulin-responsive mechanism is not present ubiquitously (16, 19, 27, 34, 38, 39, 83, 89, 107).

The situation in 3T3-L1 preadipocytes and in CHO cells is more complicated. We observed highly insulin-responsive GLUT4 trafficking, at least to some degree, in "undifferentiated" 3T3-L1 preadipocytes. The overall fold increase in GLUT4 at the cell surface is less in these cells than in day 2 3T3-L1 cells or in fully differentiated 3T3-L1 adipocytes, yet we consistently observed an overshoot of the final steady-state response in the presence of insulin (Fig. 2b, 3a, 4a, 4b, and 4c). This result does not arise from culture of the cells in fetal bovine serum rather than calf serum (Fig. 4c). We also consistently observed greater sequestration of the GLUT4 reporter on day 2 of differentiation (and subsequently) than in the undifferentiated cells (Fig. 2b and 3a). It is possible that two mechanisms are operative: one for basal sequestration that is active in 3T3-L1 adipocytes but not active in 3T3-L1 preadipocytes and another that is responsible for the overshoot that is active in both 3T3-L1 adipocytes and preadipocytes, but not in NIH 3T3 cells. However, a simpler explanation is that GLUT4 undergoes partial targeting to a highly insulin-responsive compartment in the 3T3-L1 preadipocytes, sufficient to cause the overshoot but not sufficient to cause significant basal sequestration (i.e., by drawing enough GLUT4 out of the endosomal system). We hypothesize that such a mechanism becomes more active at day 2 of differentiation and is then sufficient to deplete GLUT4 from endosomes. This would result in greater fold translocation of GLUT4 to the cell surface on day 2 because of increased sequestration in the basal state, consistent with our data. Such an interpretation might also be compatible with findings that a biochemically detectable population of highly insulin-responsive vesicles first develops in 3T3-L1 cells at 2 to 3 days after induction of differentiation (19). Of course, there is also likely to be significant variation among 3T3-L1 cell lines used in different laboratories.

The idea of partial sorting may also apply to CHO cells, which appear to possess a highly insulin-sensitive trafficking mechanism, but which do not generally translocate GLUT4 by the same fold increase seen in fully differentiated 3T3-L1 adipocytes (4, 16, 43, 44, 93). Importantly, CHO cells have several adipocyte-like features, and the observation of a highly insulin-responsive GLUT4 trafficking mechanism in these cells does not imply that such a mechanism is present in all cell types. CHO-K1 cells transfected with the β3-adrenergic receptor accumulate triglyceride droplets when cultured in differentiation medium similar to that used for 3T3-L1 cells (25). The untransfected CHO cells constitutively express hormone-sensitive lipase and peroxisome proliferator-activated receptor γ (PPARγ), a major regulator of adipose differentiation; PPARγ expression is upregulated in the presence of the β3-adrenergic receptor and differentiation medium. Thus, CHO cells have several adipocyte-like characteristics, and the notion that CHO cells can mobilize GLUT4 from an adipocyte-like, highly insulin-responsive compartment is not inconsistent with reports finding that heterogeneous expression of GLUT4 usually results in intracellular sequestration without insulin responsiveness (4, 16, 27, 34, 39, 89, 107).

Amino acid concentrations regulate GLUT4 trafficking. We hypothesize that the mechanism for sorting and retaining GLUT4 in a highly insulin-responsive compartment is somewhat less efficient in CHO cells than in 3T3-L1 adipocytes, but that it is otherwise essentially the same and that both cell types can be considered models for primary adipocytes. 3T3-L1 adipocytes are the better model, based on expression of known adipocyte marker proteins. Despite this distinction, amino acid concentrations (and rapamycin treatment) likely alter the same step(s) in the GLUT4 recycling pathway in both cell types. If so, then the simplest explanation to encompass the data that we present is that amino acid concentrations (and rapamycin) alter the rate of GLUT4 movement from the highly insulin-responsive compartment to the cell surface in both the absence and presence of insulin. In CHO cells, most GLUT4 recycles via the endosomal system. Yet in sufficient amino acids, traffic through the highly insulin-responsive compartment becomes significant and is detectable (Fig. 5 and 7). In contrast, in 3T3-L1 adipocytes, the sorting-retention machinery is efficient enough to cause some GLUT4 accumulation in—and trafficking through—a highly insulin-responsive compartment even in low concentrations of amino acids. Thus, in the presence of low amino acid concentrations or rapamycin, the overshoot remains, though the overall fold increase in cell surface GLUT4 is decreased (Fig. 9 and 10).

Our kinetic and microscopy data suggest that amino acid concentrations regulate the accumulation of GLUT4 in a peripheral, highly insulin-responsive compartment in CHO cells. Thus, in the presence of high amino acid concentrations, GLUT4 is concentrated in the periphery and insulin stimulation results in an initial, marked overshoot of the steady-state proportion of GLUT4 at the cell surface. In low amino acid concentrations, much GLUT4 remains in a perinuclear or trans-Golgi location, and the kinetics of externalization are

more modest and exhibit no overshoot of the final, steady-state response. We do not know if this peripheral, insulin-mobilizable compartment in CHO cells is the same as the highly insulin-responsive compartment in 3T3-L1 cells. Indeed, immunofluorescence microscopy in primary and cultured adipocytes suggests that TfnR-negative compartments containing GLUT4 are present both in the periphery and in a perinuclear location (7, 60, 61). Perinuclear GLUT4 may be in a storage compartment and appears to require intact actin and microtubule networks for mobilization (55, 56, 70). It may be that insulin stimulates both release of a GLUT4-tethering mechanism and fusion of vesicles containing GLUT4 with the plasma membrane and that low amino acid concentrations (or rapamycin) inhibit the latter but not the former. If such an explanation is correct, it would suggest that the peripheral vesicles that we observed in CHO cells cultured in DMEM may be docked but not fused at the plasma membrane.

That amino acid abundance (or rapamycin treatment) would secondarily regulate a step in the GLUT4 recycling pathway that is also controlled by insulin fits well with other data. Rapamycin appears to inhibit mTOR kinase activity quite specifically and mimics amino acid starvation in both yeast and mammalian cells; in *Saccharomyces cerevisiae*, Tor protein activates metabolic pathways for glucose utilization (9, 29; reviewed in reference 88). In mammalian cells, insulin is well known to signal through phosphatidylinositol-3-kinase and protein kinase B (PKB [Akt]) to phosphorylate p70 S6 kinase and eIF-4E BP1, and this effect is sensitive to both amino acid sufficiency and rapamycin (28, 58, 90, 94). Paradoxically, amino acids appear to inhibit insulin-stimulated phosphorylation of IRS-1 and IRS-2 and inhibit phosphatidylinositol-3-kinase activity (71). This latter effect may result from mTOR-mediated serine phosphorylation and subsequent proteasomal degradation of IRS proteins (30, 31, 72). A rapamycin-sensitive pathway is also important in controlling expression of the p85α regulatory subunit of phosphatidylinositol-3-kinase in muscle (80). Other data indicate that rapamycin and nutrient insufficiency decrease signaling through atypical protein kinase C (69, 115). Since both PKB and atypical protein kinase C isoforms have been implicated in regulation of GLUT4 trafficking, either or both of these pathways could be important for the response of GLUT4 to amino acid concentrations that we describe (17). Our data do not contradict previous work showing that short-term rapamycin treatment has no effect on insulin-stimulated glucose uptake (21). Rather, we find an effect of longer-term amino acid starvation or rapamycin treatment on GLUT4 distribution in unstimulated cells. Thus, it seems more likely that amino acids and rapamycin are regulating some transcriptional or translational output, which in turn alters the distribution of GLUT4 in the basal state. Further characterization of this mechanism will be the subject of much future work.

ACKNOWLEDGMENTS

We thank Zhijun Luo and Joseph Avruch for the GLUT4*myc* cDNA, Bill Schiemann for the pCS2+MT vector, Maureen Charron for antisera, and Glenn Paradis for assistance with flow cytometry and sorting. We thank Toshio Kitamura for the pMX retrovirus vector, Merav Socolovsky and Garry Nolan for retrovirus packaging cell lines, and David Hirsch, Roger Lawrence, and Monty Kreiger for the CHO cell line expressing the murine ecotropic retrovirus receptor. We thank Natalie Hendon for assistance with tissue culture and Jen Cook-Chrysos for help with figures. We thank three anonymous reviewers for helpful comments on the manuscript.

This work was supported by NIH grants K11 DK02371 to J.S.B. and R37 DK47618 to H.F.L., as well as by a grant from the American Diabetes Association to J.S.B.

REFERENCES

1. **Aledo, J. C., L. Lavoie, A. Volchuk, S. R. Keller, A. Klip, and H. S. Hundal.** 1997. Identification and characterization of two distinct intracellular GLUT4 pools in rat skeletal muscle: evidence for an endosomal and an insulin-sensitive GLUT4 compartment. Biochem. J. **325:**727–732.
2. **Al-Hasani, H., D. R. Yver, and S. W. Cushman.** 1999. Overexpression of the glucose transporter GLUT4 in adipose cells interferes with insulin-stimulated translocation. FEBS Lett. **460:**338–342.
3. **Araki, S., J. Yang, M. Hashiramoto, Y. Tamori, M. Kasuga, and G. D. Holman.** 1996. Subcellular trafficking kinetics of GLUT4 mutated at the N- and C-terminal. Biochem. J. **315:**153–159.
4. **Asano, T., K. Takata, H. Katagiri, K. Tsukuda, J. L. Lin, H. Ishihara, K. Inukai, H. Hirano, Y. Yazaki, and Y. Oka.** 1992. Domains responsible for the differential targeting of glucose transporter isoforms. J. Biol. Chem. **267:**19636–19641.
5. **Baker, B. W., D. Boettiger, E. Spooncer, and J. D. Norton.** 1992. Efficient retroviral-mediated gene transfer into human B lymphoblastoid cells expressing mouse ecotropic viral receptor. Nucleic Acids Res. **20:** 5234.
6. **Baumann, C. A., V. Ribon, M. Kanzaki, D. C. Thurmond, S. Mora, S. Shigematsu, P. E. Bickel, J. E. Pessin, and A. R. Saltiel.** 2000. CAP defines a second signalling pathway required for insulin-stimulated glucose transport. Nature **407:**202–207.
7. **Bogan, J. S., and H. F. Lodish.** 1999. Two compartments for insulin-stimulated exocytosis in 3T3-L1 adipocytes defined by endogenous ACRP30 and GLUT4. J. Cell Biol. **146:**609–620.
8. **Bradley, R. L., and B. Cheatham.** 1999. Regulation of ob gene expression and leptin secretion by insulin and dexamethasone in rat adipocytes. Diabetes **48:**272–278.
9. **Burnett, P. E., R. K. Barrow, N. A. Cohen, S. H. Snyder, and D. M. Sabatini.** 1998. RAFT1 phosphorylation of the translational regulators p70 S6 kinase and 4E-BP1. Proc. Natl. Acad. Sci. USA **95:**1432–1437.
10. **Calderhead, D. M., K. Kitagawa, L. I. Tanner, G. D. Holman, and G. E. Lienhard.** 1990. Insulin regulation of the two glucose transporters in 3T3–L1 adipocytes. J. Biol. Chem. **265:**13801–13808.
11. **Charron, M. J., F. C. Brosius III, S. L. Alper, and H. F. Lodish.** 1989. A glucose transport protein expressed predominately in insulin-responsive tissues. Proc. Natl. Acad. Sci. USA **86:**2535–2539.
12. **Charron, M. J., E. B. Katz, and A. L. Olson.** 1999. GLUT4 gene regulation and manipulation. J. Biol. Chem. **274:**3253–3256.
13. **Cheatham, B., C. J. Vlahos, L. Cheatham, L. Wang, J. Blenis, and C. R. Kahn.** 1994. Phosphatidylinositol 3-kinase activation is required for insulin stimulation of pp70 S6 kinase, DNA synthesis, and glucose transporter translocation. Mol. Cell. Biol. **14:**4902–4911.
14. **Clark, A. E., G. D. Holman, and I. J. Kozka.** 1991. Determination of the rates of appearance and loss of glucose transporters at the cell surface of rat adipose cells. Biochem. J. **278:**235–241.
15. **Cushman, S. W., and L. J. Wardzala.** 1980. Potential mechanism of insulin action on glucose transport in the isolated rat adipose cell: apparent translocation of intracellular transport systems to the plasma membrane. J. Biol. Chem. **255:**4758–4762.
16. **Czech, M. P., A. Chawla, C. W. Woon, J. Buxton, M. Armoni, W. Tang, M. Joly, and S. Corvera.** 1993. Exofacial epitope-tagged glucose transporter chimeras reveal COOH-terminal sequences governing cellular localization. J. Cell Biol. **123:**127–135.
17. **Czech, M. P., and S. Corvera.** 1999. Signaling mechanisms that regulate glucose transport. J. Biol. Chem. **274:**1865–1868.
18. **Dobson, S. P., C. Livingstone, G. W. Gould, and J. M. Tavare.** 1996. Dynamics of insulin-stimulated translocation of GLUT4 in single living cells visualised using green fluorescent protein. FEBS Lett. **393:**179–184.
19. **El-Jack, A. K., K. V. Kandror, and P. F. Pilch.** 1999. The formation of an insulin-responsive vesicular cargo compartment is an early event in 3T3-L1 adipocyte differentiation. Mol. Biol. Cell **10:**1581–1594.
20. **Filippis, A., S. Clark, and J. Proietto.** 1998. Possible role for gp160 in constitutive but not insulin-stimulated GLUT4 trafficking: dissociation of gp160 and GLUT4 localization. Biochem. J. **330:**405–411.
21. **Fingar, D. C., S. F. Hausdorff, J. Blenis, and M. J. Birnbaum.** 1993. Dissociation of pp70 ribosomal protein S6 kinase from insulin-stimulated glucose transport in 3T3-L1 adipocytes. J. Biol. Chem. **268:**3005–3008.
22. **Frost, S. C., and M. D. Lane.** 1985. Evidence for the involvement of vicinal

sulfhydryl groups in insulin-activated hexose transport by 3T3-L1 adipocytes. J. Biol. Chem. **260:**2646–2652.
23. **Garza, L. A., and M. J. Birnbaum.** 2000. Insulin-responsive aminopeptidase trafficking in 3T3-L1 adipocytes. J. Biol. Chem. **275:**2560–2567.
24. **Green, H., and O. Kehinde.** 1975. An established preadipose cell line and its differentiation in culture. II. Factors affecting the adipose conversion. Cell **5:**19–27.
25. **Gros, J., C. C. Gerhardt, and A. D. Strosberg.** 1999. Expression of human (beta)3-adrenergic receptor induces adipocyte-like features in CHO/K1 fibroblasts. J. Cell Sci. **112:**3791–3797.
26. **Gustavsson, J., S. Parpal, and P. Stralfors.** 1996. Insulin-stimulated glucose uptake involves the transition of glucose transporters to a caveolae-rich fraction within the plasma membrane: implications for type II diabetes. Mol. Med. **2:**367–372.
27. **Haney, P. M., J. W. Slot, R. C. Piper, D. E. James, and M. Mueckler.** 1991. Intracellular targeting of the insulin-regulatable glucose transporter (GLUT4) is isoform specific and independent of cell type. J. Cell Biol. **114:**689–699.
28. **Hara, K., K. Yonezawa, Q. P. Weng, M. T. Kozlowski, C. Belham, and J. Avruch.** 1998. Amino acid sufficiency and mTOR regulate p70 S6 kinase and eIF-4E BP1 through a common effector mechanism. J. Biol. Chem. **273:**14484–14494. (Erratum, **273:**22160.)
29. **Hardwick, J. S., F. G. Kuruvilla, J. K. Tong, A. F. Shamji, and S. L. Schreiber.** 1999. Rapamycin-modulated transcription defines the subset of nutrient-sensitive signaling pathways directly controlled by the Tor proteins. Proc. Natl. Acad. Sci. USA **96:**14866–14870.
30. **Hartman, M. E., M. Villela-Bach, J. Chen, and G. G. Freund.** 2001. FRAP-Dependent serine phosphorylation of IRS-1 inhibits IRS-1 tyrosine phosphorylation. Biochem. Biophys. Res. Commun. **280:**776–781.
31. **Haruta, T., T. Uno, J. Kawahara, A. Takano, K. Egawa, P. M. Sharma, J. M. Olefsky, and M. Kobayashi.** 2000. A rapamycin-sensitive pathway down-regulates insulin signaling via phosphorylation and proteasomal degradation of insulin receptor substrate-1. Mol. Endocrinol. **14:**783–794.
32. **Hashiramoto, M., and D. E. James.** 2000. Characterization of insulin-responsive GLUT4 storage vesicles isolated from 3T3–L1 adipocytes. Mol. Cell. Biol. **20:**416–427.
33. **Hausdorff, S. F., D. C. Fingar, K. Morioka, L. A. Garza, E. L. Whiteman, S. A. Summers, and M. J. Birnbaum.** 1999. Identification of wortmannin-sensitive targets in 3T3-L1 adipocytes: dissociation of insulin-stimulated glucose uptake and glut4 translocation. J. Biol. Chem. **274:**24677–24684.
34. **Herman, G. A., F. Bonzelius, A. M. Cieutat, and R. B. Kelly.** 1994. A distinct class of intracellular storage vesicles, identified by expression of the glucose transporter GLUT4. Proc. Natl. Acad. Sci. USA **91:**12750–12754.
35. **Holman, G. D., and S. W. Cushman.** 1996. Subcellular trafficking of GLUT4 in insulin target cells. Semin. Cell Dev. Biol. **7:**259–268.
36. **Holman, G. D., I. J. Kozka, A. E. Clark, C. J. Flower, J. Saltis, A. D. Habberfield, I. A. Simpson, and S. W. Cushman.** 1990. Cell surface labeling of glucose transporter isoform GLUT4 by bis-mannose photolabel: correlation with stimulation of glucose transport in rat adipose cells by insulin and phorbol ester. J. Biol. Chem. **265:**18172–18179.
37. **Holman, G. D., L. Lo Leggio, and S. W. Cushman.** 1994. Insulin-stimulated GLUT4 glucose transporter recycling: a problem in membrane protein subcellular trafficking through multiple pools. J. Biol. Chem. **269:**17516–17524.
38. **Hudson, A. W., D. C. Fingar, G. A. Seidner, G. Griffiths, B. Burke, and M. J. Birnbaum.** 1993. Targeting of the "insulin-responsive" glucose transporter (GLUT4) to the regulated secretory pathway in PC12 cells. J. Cell Biol. **122:**579–588.
39. **Hudson, A. W., M. Ruiz, and M. J. Birnbaum.** 1992. Isoform-specific subcellular targeting of glucose transporters in mouse fibroblasts. J. Cell Biol. **116:**785–797.
40. **Ishii, K., H. Hayashi, M. Todaka, S. Kamohara, F. Kanai, H. Jinnouchi, L. Wang, and Y. Ebina.** 1995. Possible domains responsible for intracellular targeting and insulin-dependent translocation of glucose transporter type 4. Biochem. J. **309:**813–823.
41. **Jhun, B. H., A. L. Rampal, H. Liu, M. Lachaal, and C. Y. Jung.** 1992. Effects of insulin on steady state kinetics of GLUT4 subcellular distribution in rat adipocytes: evidence of constitutive GLUT4 recycling. J. Biol. Chem. **267:**17710–17715.
42. **Jiang, T., G. Sweeney, M. T. Rudolf, A. Klip, A. Traynor-Kaplan, and R. Y. Tsien.** 1998. Membrane-permeant esters of phosphatidylinositol 3,4,5-trisphosphate. J. Biol. Chem. **273:**11017–11024.
43. **Johnson, A. O., A. Subtil, R. Petrush, K. Kobylarz, S. R. Keller, and T. E. McGraw.** 1998. Identification of an insulin-responsive, slow endocytic recycling mechanism in Chinese hamster ovary cells. J. Biol. Chem. **273:**17968–17977.
44. **Kanai, F., Y. Nishioka, H. Hayashi, S. Kamohara, M. Todaka, and Y. Ebina.** 1993. Direct demonstration of insulin-induced GLUT4 translocation to the surface of intact cells by insertion of a c-*myc* epitope into an exofacial GLUT4 domain. J. Biol. Chem. **268:**14523–14526.
45. **Kandror, K. V.** 1999. Insulin regulation of protein traffic in rat adipose cells. J. Biol. Chem. **274:**25210–25217.
46. **Kandror, K. V., and P. F. Pilch.** 1998. Multiple endosomal recycling pathways in rat adipose cells. Biochem. J. **331:**829–835.
47. **Kandror, K. V., J. M. Stephens, and P. F. Pilch.** 1995. Expression and compartmentalization of caveolin in adipose cells: coordinate regulation with and structural segregation from GLUT4. J. Cell Biol. **129:**999–1006.
48. **Kao, A. W., B. P. Ceresa, S. R. Santeler, and J. E. Pessin.** 1998. Expression of a dominant interfering dynamin mutant in 3T3L1 adipocytes inhibits GLUT4 endocytosis without affecting insulin signaling. J. Biol. Chem. **273:**25450–25457.
49. **Karnieli, E., M. J. Zarnowski, P. J. Hissin, I. A. Simpson, L. B. Salans, and S. W. Cushman.** 1981. Insulin-stimulated translocation of glucose transport systems in the isolated rat adipose cell: time course, reversal, insulin concentration dependency, and relationship to glucose transport activity. J. Biol. Chem. **256:**4772–4777.
50. **Katagiri, H., T. Asano, H. Ishihara, K. Inukai, Y. Shibasaki, M. Kikuchi, Y. Yazaki, and Y. Oka.** 1996. Overexpression of catalytic subunit p110alpha of phosphatidylinositol 3-kinase increases glucose transport activity with translocation of glucose transporters in 3T3-L1 adipocytes. J. Biol. Chem. **271:**16987–16990.
51. **Kinoshita, S., B. K. Chen, H. Kaneshima, and G. P. Nolan.** 1998. Host control of HIV-1 parasitism in T cells by the nuclear factor of activated T cells. Cell **95:**595–604.
52. **Kohanski, R. A., S. C. Frost, and M. D. Lane.** 1986. Insulin-dependent phosphorylation of the insulin receptor-protein kinase and activation of glucose transport in 3T3-L1 adipocytes. J. Biol. Chem. **261:**12272–12281.
53. **Kuroda, M., R. C. Honnor, S. W. Cushman, C. Londos, and I. A. Simpson.** 1987. Regulation of insulin-stimulated glucose transport in the isolated rat adipocyte: cAMP-independent effects of lipolytic and antilipolytic agents. J. Biol. Chem. **262:**245–253.
54. **Lampson, M. A., A. Racz, S. W. Cushman, and T. E. McGraw.** 2000. Demonstration of insulin-responsive trafficking of GLUT4 and vpTR in fibroblasts. J. Cell Sci. **113:**4065–4076.
55. **Lee, W., J. Ryu, R. P. Souto, P. F. Pilch, and C. Y. Jung.** 1999. Separation and partial characterization of three distinct intracellular GLUT4 compartments in rat adipocytes: subcellular fractionation without homogenization. J. Biol. Chem. **274:**37755–37762.
56. **Lee, W., J. Ryu, R. A. Spangler, and C. Y. Jung.** 2000. Modulation of GLUT4 and GLUT1 recycling by insulin in rat adipocytes: kinetic analysis based on the involvement of multiple intracellular compartments. Biochemistry **39:**9358–9366.
57. **Livingstone, C., D. E. James, J. E. Rice, D. Hanpeter, and G. W. Gould.** 1996. Compartment ablation analysis of the insulin-responsive glucose transporter (GLUT4) in 3T3-L1 adipocytes. Biochem. J. **315:**487–495.
58. **Long, W., L. Saffer, L. Wei, and E. J. Barrett.** 2000. Amino acids regulate skeletal muscle PHAS-I and p70 S6-kinase phosphorylation independently of insulin. Am. J. Physiol. Endocrinol. Metab. **279:**E301–E306.
59. **Macaulay, S. L., D. R. Hewish, K. H. Gough, V. Stoichevska, S. F. MacPherson, M. Jagadish, and C. W. Ward.** 1997. Functional studies in 3T3L1 cells support a role for SNARE proteins in insulin stimulation of GLUT4 translocation. Biochem. J. **324:**217–224.
60. **Malide, D., and S. W. Cushman.** 1997. Morphological effects of wortmannin on the endosomal system and GLUT4-containing compartments in rat adipose cells. J. Cell Sci. **110:**2795–2806.
61. **Malide, D., N. K. Dwyer, E. J. Blanchette-Mackie, and S. W. Cushman.** 1997. Immunocytochemical evidence that GLUT4 resides in a specialized translocation post-endosomal VAMP2-positive compartment in rat adipose cells in the absence of insulin. J. Histochem. Cytochem. **45:**1083–1096.
62. **Malide, D., J. F. St-Denis, S. R. Keller, and S. W. Cushman.** 1997. vp165 and GLUT4 share similar vesicle pools along their trafficking pathways in rat adipose cells. FEBS Lett. **409:**461–468.
63. **Marsh, B. J., R. A. Alm, S. R. McIntosh, and D. E. James.** 1995. Molecular regulation of GLUT-4 targeting in 3T3–L1 adipocytes. J. Cell Biol. **130:**1081–1091.
64. **Martin, S., C. A. Millar, C. T. Lyttle, T. Meerloo, B. J. Marsh, G. W. Gould, and D. E. James.** 2000. Effects of insulin on intracellular GLUT4 vesicles in adipocytes: evidence for a secretory mode of regulation. J. Cell Sci. **113**(Pt. 19)**:**3427–3438.
65. **Martin, S., J. E. Rice, G. W. Gould, S. R. Keller, J. W. Slot, and D. E. James.** 1997. The glucose transporter GLUT4 and the aminopeptidase vp165 colocalise in tubulo-vesicular elements in adipocytes and cardiomyocytes. J. Cell Sci. **110:**2281–2291.
66. **Melvin, D. R., B. J. Marsh, A. R. Walmsley, D. E. James, and G. W. Gould.** 1999. Analysis of amino and carboxy terminal GLUT-4 targeting motifs in 3T3–L1 adipocytes using an endosomal ablation technique. Biochemistry **38:**1456–1462.
67. **Oatey, P. B., D. H. Van Weering, S. P. Dobson, G. W. Gould, and J. M.**

Tavare. 1997. GLUT4 vesicle dynamics in living 3T3 L1 adipocytes visualized with green-fluorescent protein. Biochem. J. **327:**637–642.
68. **Onishi, M., S. Kinoshita, Y. Morikawa, A. Shibuya, J. Phillips, L. L. Lanier, D. M. Gorman, G. P. Nolan, A. Miyajima, and T. Kitamura.** 1996. Applications of retrovirus-mediated expression cloning. Exp. Hematol. **24:**324–329.
69. **Parekh, D., W. Ziegler, K. Yonezawa, K. Hara, and P. J. Parker.** 1999. Mammalian TOR controls one of two kinase pathways acting upon nPKC-delta and nPKCepsilon. J. Biol. Chem. **274:**34758–34764.
70. **Patki, V. V., J. Buxton, A. Chawla, L. Lifshitz, K. Fogarty, W. Carrington, R. Tuft, and S. Corvera.** 2001. Insulin action on GLUT4 traffic visualized in single 3T3-L1 adipocytes by using ultra-fast microscopy. Mol. Biol. Cell **12:**129–141.
71. **Patti, M. E., E. Brambilla, L. Luzi, E. J. Landaker, and C. R. Kahn.** 1998. Bidirectional modulation of insulin action by amino acids. J. Clin. Investig. **101:**1519–1529.
72. **Pederson, T. M., D. L. Kramer, and C. M. Rondinone.** 2001. Serine/threonine phosphorylation of IRS-1 triggers its degradation: possible regulation by tyrosine phosphorylation. Diabetes **50:**24–31.
73. **Pessin, J. E., D. C. Thurmond, J. S. Elmendorf, K. J. Coker, and S. Okada.** 1999. Molecular basis of insulin-stimulated GLUT4 vesicle trafficking: location! location! location! J. Biol. Chem. **274:**2593–2596.
74. **Piper, R. C., L. J. Hess, and D. E. James.** 1991. Differential sorting of two glucose transporters expressed in insulin-sensitive cells. Am. J. Physiol. **260:**C570–C580.
75. **Quon, M. J., M. Guerre-Millo, M. J. Zarnowski, A. J. Butte, M. Em, S. W. Cushman, and S. I. Taylor.** 1994. Tyrosine kinase-deficient mutant human insulin receptors (Met1153→Ile) overexpressed in transfected rat adipose cells fail to mediate translocation of epitope-tagged GLUT4. Proc. Natl. Acad. Sci. USA **91:**5587–5591.
76. **Ramm, G., J. W. Slot, D. E. James, and W. Stoorvogel.** 2000. Insulin recruits GLUT4 from specialized VAMP2-carrying vesicles as well as from the dynamic endosomal/trans-Golgi network in rat adipocytes. Mol. Biol. Cell **11:**4079–4091.
77. **Rea, S., and D. E. James.** 1997. Moving GLUT4: the biogenesis and trafficking of GLUT4 storage vesicles. Diabetes **46:**1667–1677.
78. **Reed, B. C., and M. D. Lane.** 1980. Insulin receptor synthesis and turnover in differentiating 3T3–L1 preadipocytes. Proc. Natl. Acad. Sci. USA **77:**285–289.
79. **Robinson, L. J., S. Pang, D. S. Harris, J. Heuser, and D. E. James.** 1992. Translocation of the glucose transporter (GLUT4) to the cell surface in permeabilzed 3T3–L1 adipocytes: effects of ATP, insulin, and GTPγS and localization of GLUT4 to clathrin lattices. J. Cell Biol. **117:**1181–1196.
80. **Roques, M., and H. Vidal.** 1999. A phosphatidylinositol 3-kinase/p70 ribosomal S6 protein kinase pathway is required for the regulation by insulin of the p85alpha regulatory subunit of phosphatidylinositol 3-kinase gene expression in human muscle cells. J. Biol. Chem. **274:**34005–34010.
81. **Ross, S. A., J. J. Herbst, S. R. Keller, and G. E. Lienhard.** 1997. Trafficking kinetics of the insulin-regulated membrane aminopeptidase in 3T3-L1 adipocytes. Biochem. Biophys. Res. Commun. **239:**247–251.
82. **Ross, S. A., S. R. Keller, and G. E. Lienhard.** 1998. Increased intracellular sequestration of the insulin-regulated aminopeptidase upon differentiation of 3T3–L1 cells. Biochem. J. **330:**1003–1008.
83. **Ross, S. A., H. M. Scott, N. J. Morris, W. Y. Leung, F. Mao, G. E. Lienhard, and S. R. Keller.** 1996. Characterization of the insulin-regulated membrane aminopeptidase in 3T3-L1 adipocytes. J. Biol. Chem. **271:**3328–3332.
84. **Saltiel, A. R.** 2001. New perspectives into the molecular pathogenesis and treatment of type 2 diabetes. Cell **104:**517–529.
85. **Satoh, S., H. Nishimura, A. E. Clark, I. J. Kozka, S. J. Vannucci, I. A. Simpson, M. J. Quon, S. W. Cushman, and G. D. Holman.** 1993. Use of bismannose photolabel to elucidate insulin-regulated GLUT4 subcellular trafficking kinetics in rat adipose cells: evidence that exocytosis is a critical site of hormone action. J. Biol. Chem. **268:**17820–17829.
86. **Scherer, P. E., M. P. Lisanti, G. Baldini, M. Sargiacomo, C. C. Mastick, and H. F. Lodish.** 1994. Induction of caveolin during adipogenesis and association of GLUT4 with caveolin-rich vesicles. J. Cell Biol. **127:**1233–1243.
87. **Scherer, P. E., S. Williams, M. Fogliano, G. Baldini, and H. F. Lodish.** 1995. A novel serum protein similar to C1q, produced exclusively in adipocytes. J. Biol. Chem. **270:**26746–26749.
88. **Schmelzle, T., and M. N. Hall.** 2000. TOR, a central controller of cell growth. Cell **103:**253–262.
89. **Schurmann, A., I. Monden, H. G. Joost, and K. Keller.** 1992. Subcellular distribution and activity of glucose transporter isoforms GLUT1 and GLUT4 transiently expressed in COS-7 cells. Biochim. Biophys. Acta **1131:**245–252.
90. **Scott, P. H., G. J. Brunn, A. D. Kohn, R. A. Roth, and J. C. Lawrence.** 1998. Evidence of insulin-stimulated phosphorylation and activation of the mammalian target of rapamycin mediated by a protein kinase B signaling pathway. Proc. Natl. Acad. Sci. USA **95:**7772–7777.
91. **Shao, D., and M. A. Lazar.** 1997. Peroxisome proliferator activated receptor gamma, CCAAT/enhancer-binding protein alpha, and cell cycle status regulate the commitment to adipocyte differentiation. J. Biol. Chem. **272:**21473–21478.
92. **Shapiro, L., and P. E. Scherer.** 1998. The crystal structure of a complement-1q family protein suggests an evolutionary link to tumor necrosis factor. Curr. Biol. **8:**335–338.
93. **Shibasaki, Y., T. Asano, J. L. Lin, K. Tsukuda, H. Katagiri, H. Ishihara, Y. Yazaki, and Y. Oka.** 1992. Two glucose transporter isoforms are sorted differentially and are expressed in distinct cellular compartments. Biochem. J. **281:**829–834.
94. **Shigemitsu, K., Y. Tsujishita, K. Hara, M. Nanahoshi, J. Avruch, and K. Yonezawa.** 1999. Regulation of translational effectors by amino acid and mammalian target of rapamycin signaling pathways: possible involvement of autophagy in cultured hepatoma cells. J. Biol. Chem. **274:**1058–1065.
95. **Simpson, F., J. P. Whitehead, and D. E. James.** 2001. GLUT4—at the crossroads between membrane trafficking and signal transduction. Traffic **2:**2–11.
96. **Slot, J. W., H. J. Geuze, S. Gigengack, D. E. James, and G. E. Lienhard.** 1991. Translocation of the glucose transporter GLUT4 in cardiac myocytes of the rat. Proc. Natl. Acad. Sci. USA **88:**7815–7819.
97. **Slot, J. W., H. J. Geuze, S. Gigengack, G. E. Lienhard, and D. E. James.** 1991. Immuno-localization of the insulin regulatable glucose transporter in brown adipose tissue of the rat. J. Cell Biol. **113:**123–135.
98. **Smith, R. M., M. J. Charron, N. Shah, H. F. Lodish, and L. Jarett.** 1991. Immunoelectron microscopic demonstration of insulin-stimulated translocation of glucose transporters to the plasma membrane of isolated rat adipocytes and masking of the carboxyl-terminal epitope of intracellular GLUT4. Proc. Natl. Acad. Sci. USA **88:**6893–6897.
99. **Socolovsky, M., I. Dusanter-Fourt, and H. F. Lodish.** 1997. The prolactin receptor and severely truncated erythropoietin receptors support differentiation of erythroid progenitors. J. Biol. Chem. **272:**14009–14012.
100. **Subtil, A., M. A. Lampson, S. R. Keller, and T. E. McGraw.** 2000. Characterization of the insulin-regulated endocytic recycling mechanism in 3T3–L1 adipocytes using a novel reporter molecule. J. Biol. Chem. **275:**4787–4795.
101. **Sumitani, S., T. Ramlal, R. Somwar, S. R. Keller, and A. Klip.** 1997. Insulin regulation and selective segregation with glucose transporter-4 of the membrane aminopeptidase vp165 in rat skeletal muscle cells. Endocrinology **138:**1029–1034.
102. **Suzuki, K., and T. Kono.** 1980. Evidence that insulin causes translocation of glucose transport activity to the plasma membrane from an intracellular storage site. Proc. Natl. Acad. Sci. USA **77:**2542–2545.
103. **Swift, S. E., J. B. Lorens, P. Achacoso, and G. P. Nolan.** 1998. Rapid production of retroviruses for efficient gene delivery to mammalian cells using 293T cell-based systems, p. 10.17.14–10.17.29. *In* J. E. Coligan, A. M. Kruisbeek, D. H. Margulies, E. M. Shevach, and W. Strober (ed.), Current protocols in immunology, vol. 2. John Wiley and Sons, Inc., New York, N.Y.
104. **Thurmond, D. C., B. P. Ceresa, S. Okada, J. S. Elmendorf, K. Coker, and J. E. Pessin.** 1998. Regulation of insulin-stimulated GLUT4 translocation by Munc18c in 3T3L1 adipocytes. J. Biol. Chem. **273:**33876–33883.
105. **Todaka, M., H. Hayashi, T. Imanaka, Y. Mitani, S. Kamohara, K. Kishi, K. Tamaoka, F. Kanai, M. Shichiri, N. Morii, S. Narumiya, and Y. Ebina.** 1996. Roles of insulin, guanosine 5′-[gamma-thio]triphosphate and phorbol 12-myristate 13-acetate in signalling pathways of GLUT4 translocation. Biochem. J. **315:**875–882.
106. **Vannucci, S. J., H. Nishimura, S. Satoh, S. W. Cushman, G. D. Holman, and I. A. Simpson.** 1992. Cell surface accessibility of GLUT4 glucose transporters in insulin-stimulated rat adipose cells: modulation by isoprenaline and adenosine. Biochem. J. **288:**325–330.
107. **Verhey, K. J., S. F. Hausdorff, and M. J. Birnbaum.** 1993. Identification of the carboxy terminus as important for the isoform-specific subcellular targeting of glucose transporter proteins. J. Cell Biol. **123:**137–147.
108. **Wang, Q., Z. Khayat, K. Kishi, Y. Ebina, and A. Klip.** 1998. GLUT4 translocation by insulin in intact muscle cells: detection by a fast and quantitative assay. FEBS Lett. **427:**193–197.
109. **Wei, M. L., F. Bonzelius, R. M. Scully, R. B. Kelly, and G. A. Herman.** 1998. GLUT4 and transferrin receptor are differentially sorted along the endocytic pathway in CHO cells. J. Cell Biol. **140:**565–575.
110. **Wu, J. C., G. Merlino, and N. Fausto.** 1994. Establishment and characterization of differentiated, nontransformed hepatocyte cell lines derived from mice transgenic for transforming growth factor alpha. Proc. Natl. Acad. Sci. USA **91:**674–678.
111. **Yang, J., A. E. Clark, R. Harrison, I. J. Kozka, and G. D. Holman.** 1992. Trafficking of glucose transporters in 3T3-L1 cells: inhibition of trafficking by phenylarsine oxide implicates a slow dissociation of transporters from

trafficking proteins. Biochem. J. **281:**809–817.
112. **Yang, J., A. E. Clark, I. J. Kozka, S. W. Cushman, and G. D. Holman.** 1992. Development of an intracellular pool of glucose transporters in 3T3-L1 cells. J. Biol. Chem. **267:**10393–10399.
113. **Yang, J., and G. D. Holman.** 1993. Comparison of GLUT4 and GLUT1 subcellular trafficking in basal and insulin-stimulated 3T3-L1 cells. J. Biol. Chem. **268:**4600–4603.
114. **Yeh, J. I., K. J. Verhey, and M. J. Birnbaum.** 1995. Kinetic analysis of glucose transporter trafficking in fibroblasts and adipocytes. Biochemistry **34:**15523–15531.
115. **Ziegler, W. H., D. B. Parekh, J. A. Le Good, R. D. Whelan, J. J. Kelly, M. Frech, B. A. Hemmings, and P. J. Parker.** 1999. Rapamycin-sensitive phosphorylation of PKC on a carboxy-terminal site by an atypical PKC complex. Curr. Biol. **9:**522–529.